CEC/ICMC 2015
CRYOGENIC ENGINEERING CONFERENCE &
INTERNATIONAL CRYOGENIC MATERIALS CONFERENCE
JW Marriott Starr Pass Resort & Spa · Tucson, Arizona, USA
June 28 – July 2, 2015

Structure and properties of oxygen-containing thin films and bulk MgB_2

T Prikhna [1], A Shapovalov [1], V Shaternik [2], M Eisterer [3], W Goldacker [4], A Kozyrev [1], M Belogolovskiy [2], H W Weber [3], M Karpets[1], V. Kovylaev[1]

[1] *Institute for Superhard Materials of the National Academy of Sciences of Ukraine, Kiev 04074, Ukraine*

[2] *G.V. Kurdyumov Institute for Metal Physics, 03680 Kyiv, Ukraine*

[3] *Atominstitut, Vienna University of Technology, Stadionallee 2, 1020 Wien, Austria*

[4] *Karlsruhe Institute of Technology (KIT), 76344 Eggenstein, Germany*

Abstract

Motivation

Despite MgB_2 is oxygen-free superconductor the high affinity of Mg toward oxygen makes practically impossible to synthesize MgB_2-based materials free of oxygen.

The structural Auger spectroscopy study of MgB_2 thin (140 nm) oxygen-containing polycrystalline films obtained by magnetron sputtering with j_c(0-1T, 20K)=7.8-2.7 MA/cm^2

and 99% dense MgB_2 bulks synthesized at 2 GPa
having j_c(0-1 T, 20 K)=0.9 – 0.7 MA/cm^2 or 0.4-0.3 MA/cm^2 (depending on initial boron),
up to 80% connectivity,
containing up to 94% of shielding fraction

allows to conclude that j_c of MgB_2 to high extend depends on distribution of admixture oxygen.

$Mg(B,O)_2$ precipitation in MgB_2 (X. Z. Liao et al. J. Appl. Phys. 93, 6208 (2003)

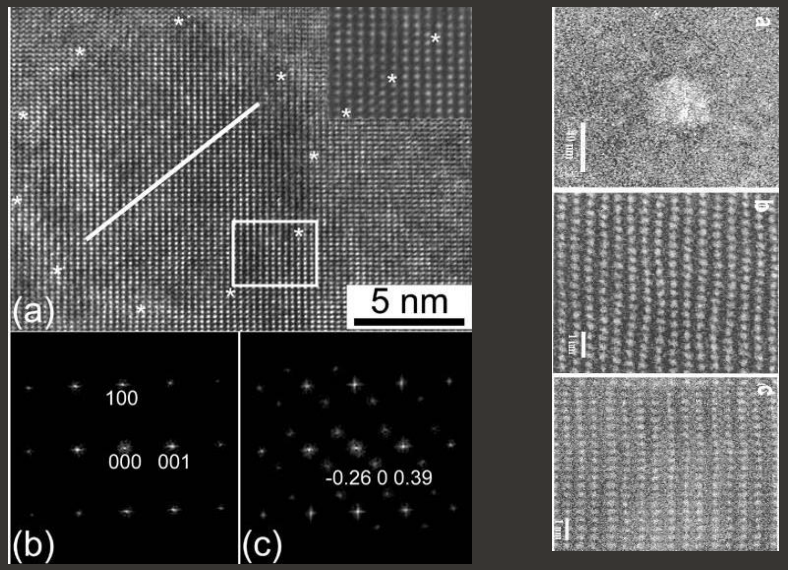

(a) An HREM image along [010] direction.

(b) Fourier transformation of the matrix.
(c) Fourier transformation of the precipitate showing satellite spots with a vector of [-0.26, 0, 0.39]

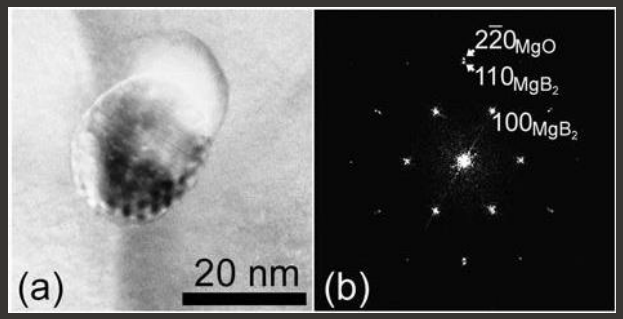

Longer exposure to trace amount of O at high temperatures also results in the transformation of the precipitates from the hexagonal $Mg(B,O)_2$ phase with compositional modulations to the face-centered cubic MgO phase.

MgB_2 grains to form coherently ordered $MgB_{2-x}O_x$ precipitates from about 5 up to 100 nm in size and that such precipitates can act as pinning centers

Ordered replacement of B atoms by O and have the same basic structure as the MgB_2 matrix but with composition modulations.

No difference in the lattice parameters between the precipitates and the matrix can be detected in conventional electron diffraction patterns.

However, extra satellite diffraction spots were revealed by HREM study in some directions implying a structural modulation caused by the precipitates.

The periodicity of O atom ordering depends on the concentration of O atoms in the precipitate and primarily occurred in the (010) plane.

Methods of preparation

Magnetron sputtering of MgB_2 thin film

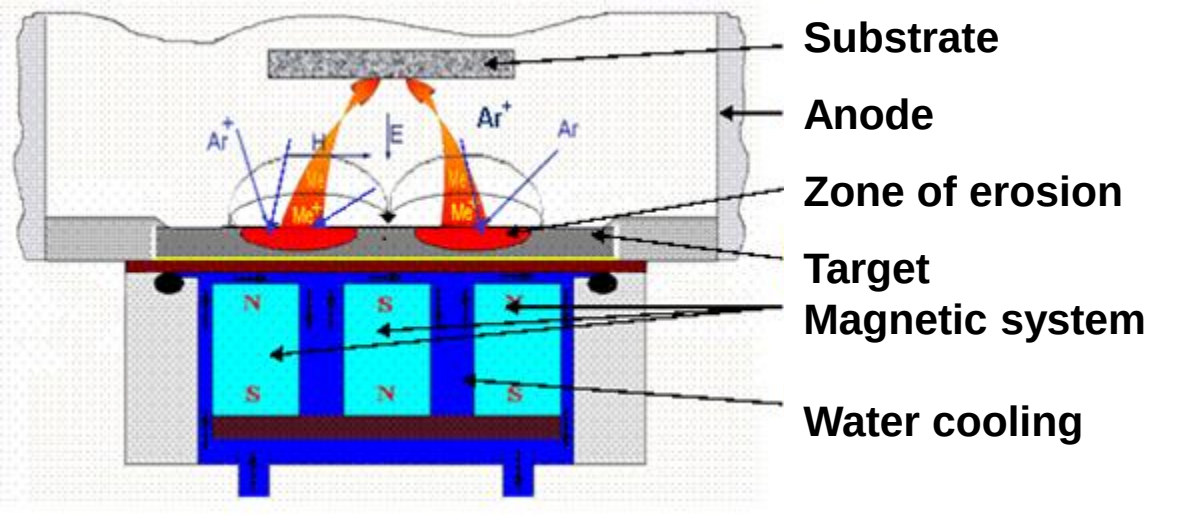

The thin MgB_2 films were deposited by DC magnetron sputtering under 1 Pa Ar pressure on 8×8×0.2 mm^3 sized substrates from leucosapphire in (0001) orientation having room temperature, which subsequently were annealed at 600-650 ^oC for 5 min in Ar under 10 Pa. For deposition we used MgB_2 target synthesized by hot pressing at 30 MPa, 800 ^oC, 1 h form Mg turning (Technical Specification of Ukraine 48-10-93-88) and commercially available precursor B powders HC Starck (grain size 4 μm, 1.5 wt% O, 0.47 wt% C, 0.40 wt% N, 0.37 wt% H).

Methods of preparation

High pressure (2 GPa) and hot pressure (30 MPa) synthesis of bulk MgB_2

ASEA (Sweeden) 140 MN effort

Recessed-anvil-type high-pressure appatatus (HPA)

Hot – P = Hot-pressing
30 MPa (300 atm)

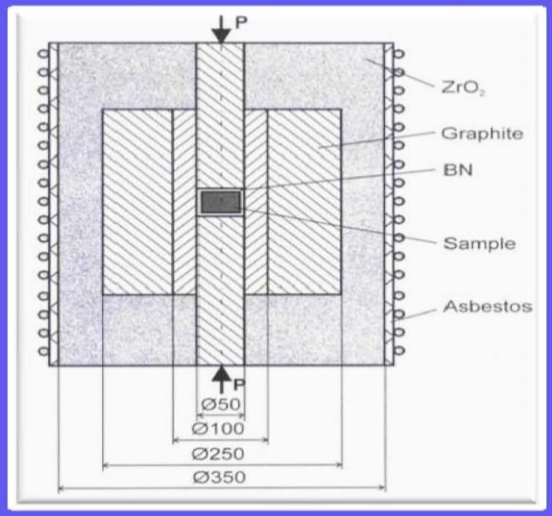

Possibility to press blocks up to 200 mm in diameter

Structure of MgB_2 thin (140 nm) film deposited by magnetron sputtering (Type 1)

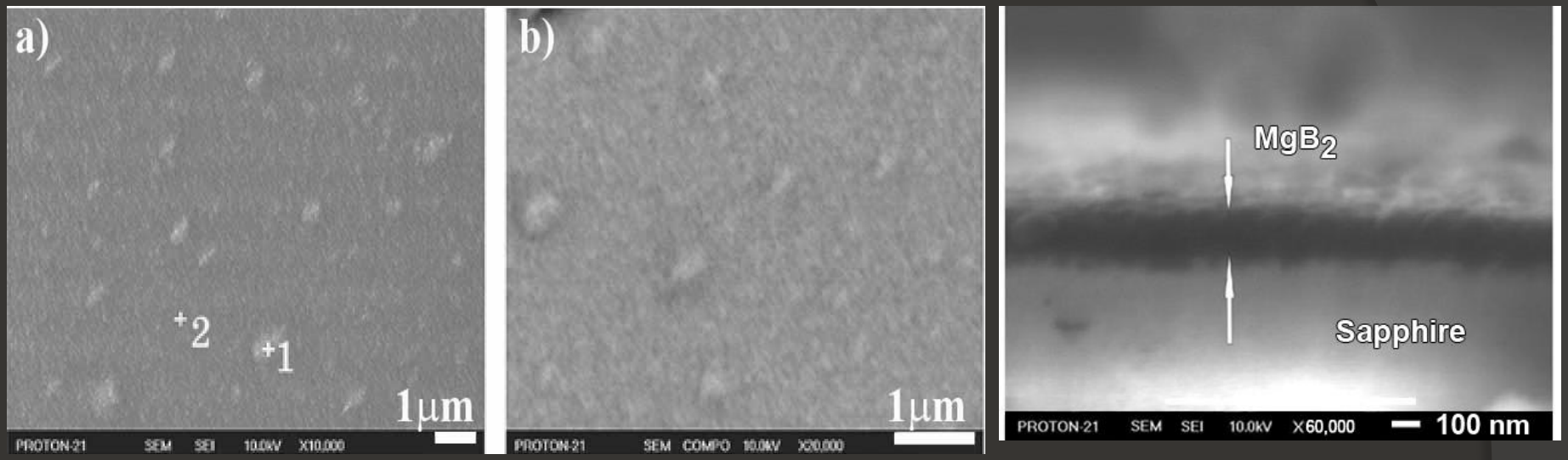

Structure of MgB_2 film after etching in Ar of oxidized surface layer in Auger spectrometer JAMP−9500F
(a) – SEI (secondary electron image showing the relief of the film) and
(b) –COMPO (compositional electron image – the brightness increase with increase in Z)

Composition (Fig.a, at.%)

in point 1: 47.9 % B, 7.1 % C, 31.6 % O, 13.4 % Mg.
and in point 2: 58.3 % B, 10.8 % C, 16.6 % O, 14.3 % Mg.

The structure of film Type 1 which demonstrates the highest *Jc* contains 16.6-31.6 at% of oxygen and nanostructural inhomogenities which can be pinning centers influencing *Jc* are much smaller and more homogeneously distributed as compare to bulk MgB_2

Critical current density, j_c, vs. magnetic field, B, of thin MgB_2 film (Type 1)

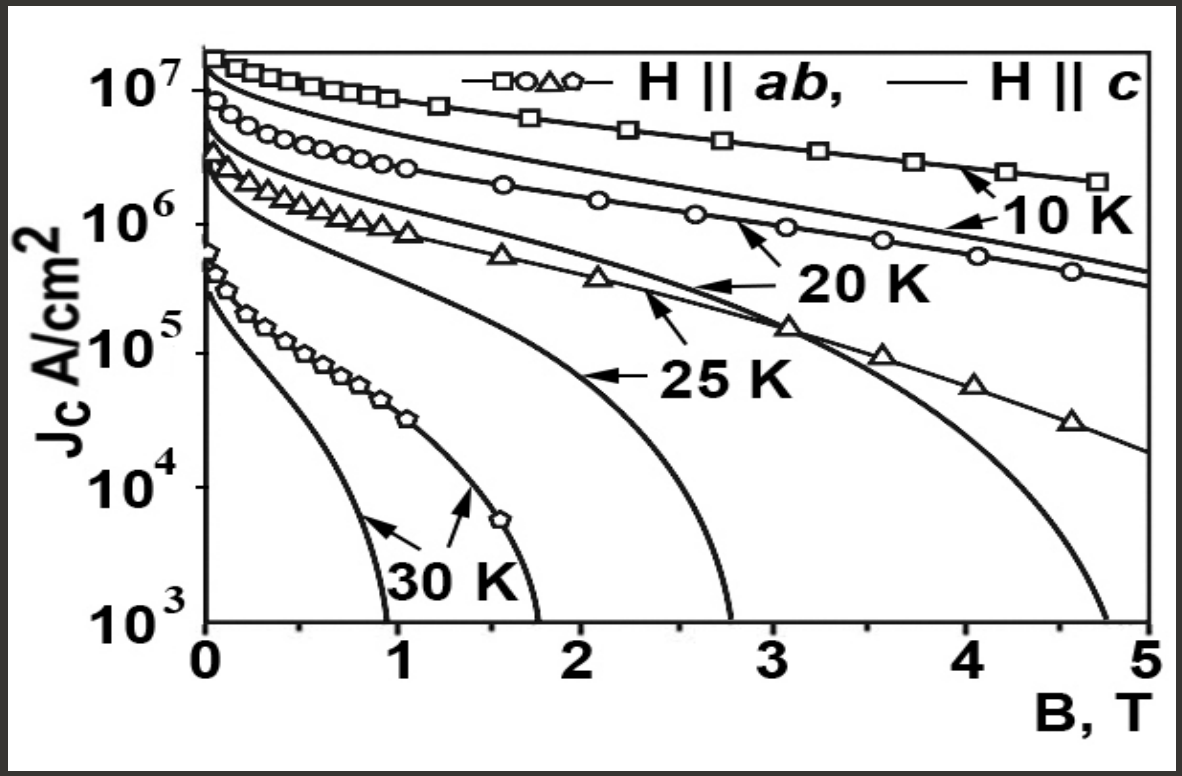

field parallel ($H||ab$) and perpendicular ($H|c$) to the substrate surface

j_c(0-1T, 20K)=7.8-2.7 MA/cm^2

The thin MgB_2 films were deposited by DC magnetron sputtering under 1 Pa Ar pressure on 8×8×0.2 mm^3 sized substrates from leucosapphire in (0001) orientation having room temperature, which subsequently were annealed at 600-650 ^oC for 5 min in Ar under 10 Pa (Type 1)

Critical current density, j_c, vs. magnetic field, B, of thin MgB_2 films after repeated annealing

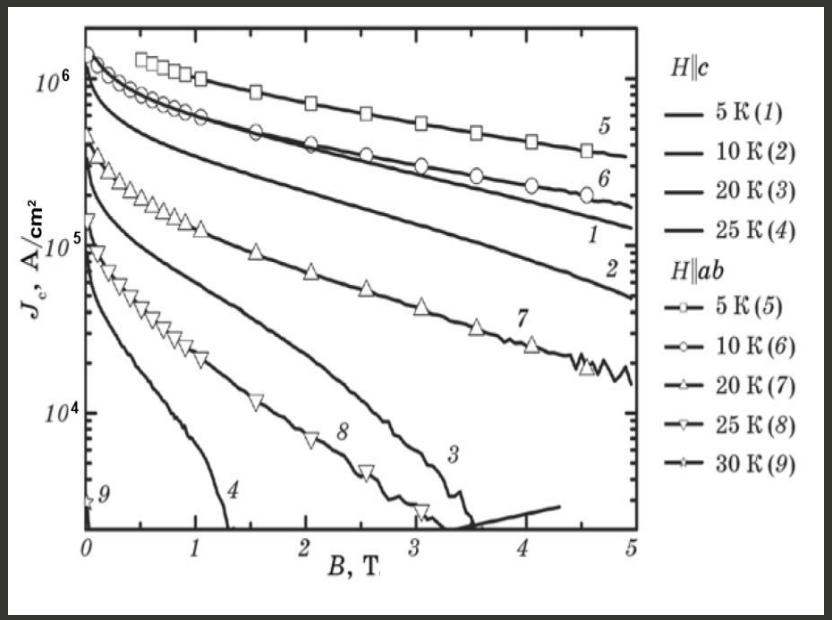

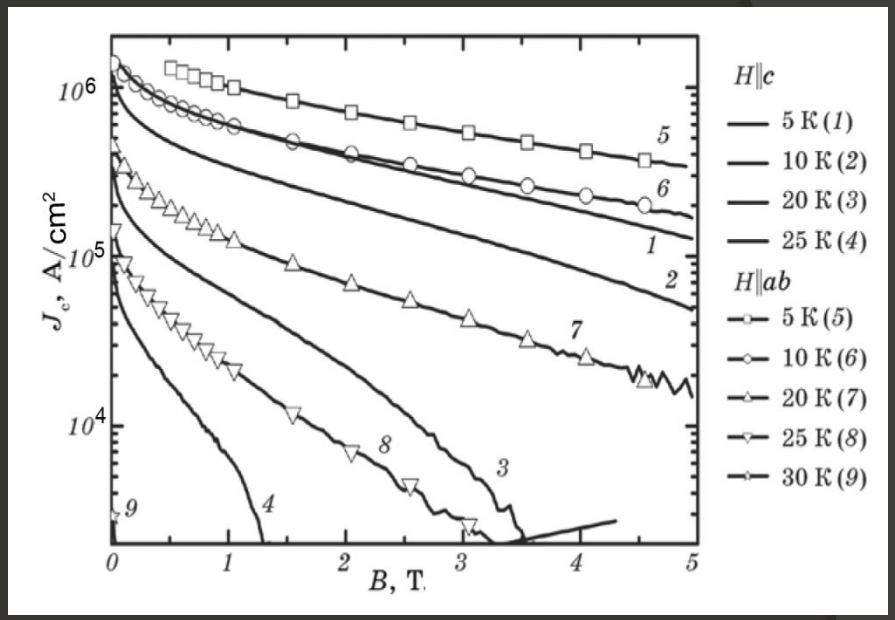

Type 2 repetedly annealed at *720—750°C for* 7 min in Mg vapor at *P = 100 Pa*

Type 3 repetedly annealed at *720—750°C for* 7 min vacuumed under *P = 0.1 Pa.*

X-ray diffraction patterns of three types thin films

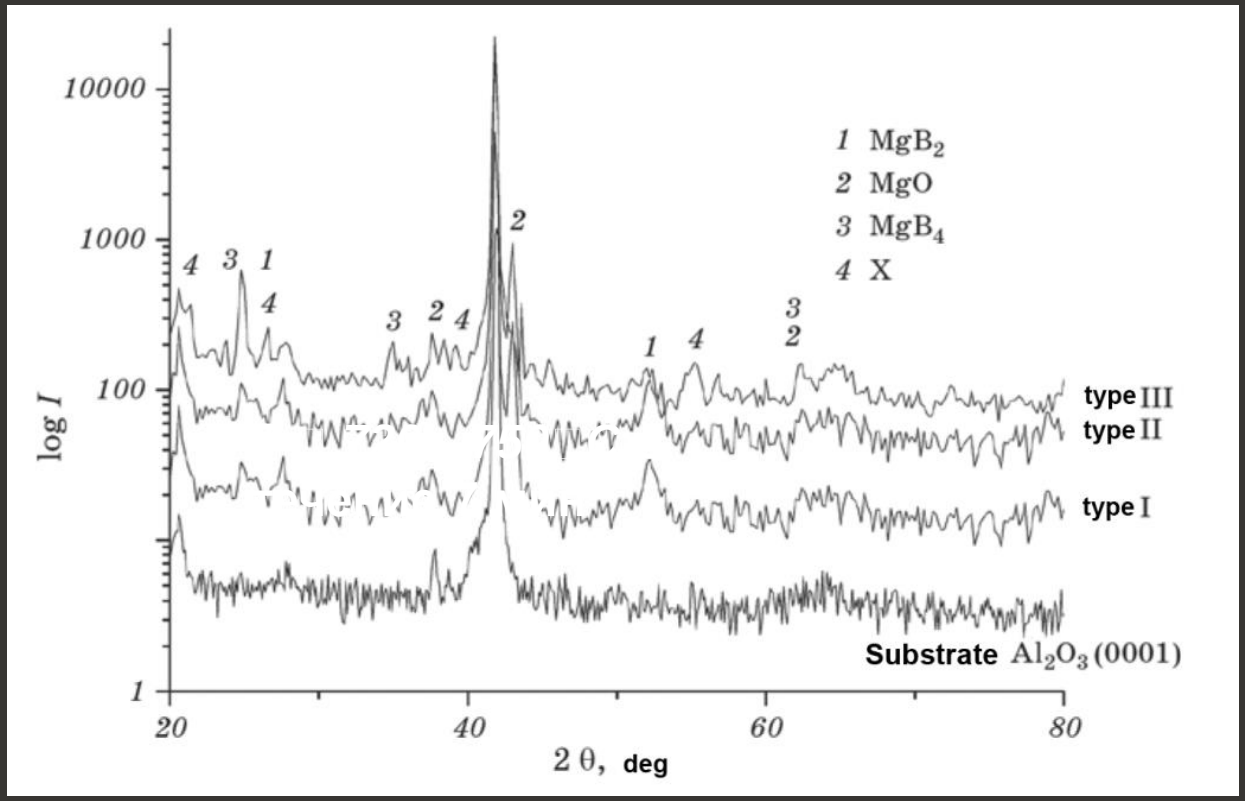

X-ray of films deposited on substrates from leucosapphire in (0001) orientation having room temperature and then heated up to 600-650 °C for 5 min under 10 Pa of Ar (Type 1) and films which after this y were repitedly annealed *at 720—750 °C for* 7 min in Mg vapor at *P = 100 Pa* (Type 2) and in 0.1 Pa vacuum (Type 3)

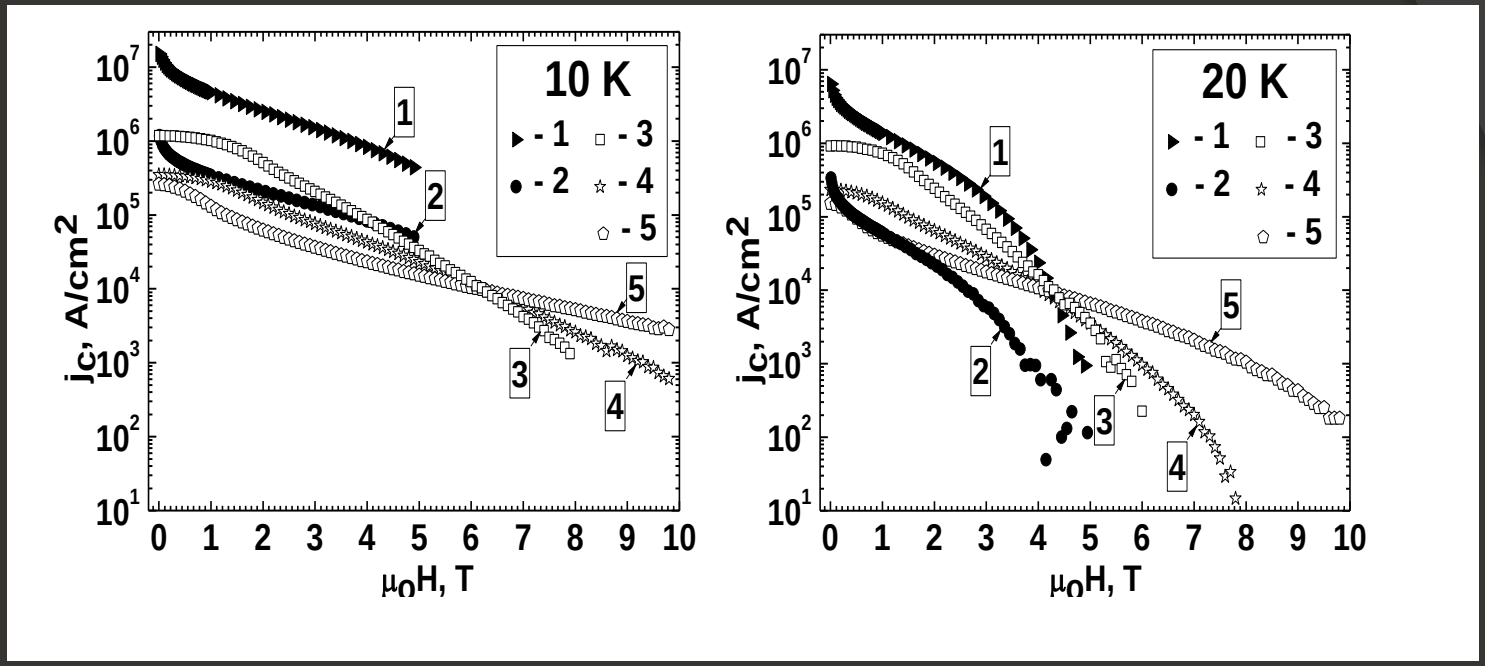

Critical current density, J_c, vs. magnetic field, $m_o H$, for thin films and bulk MgB_2:
1 – film as deposited in Ar from MgB_2 target (Type 1),
2 – the same film after repeated annealing in vacuum (Type 3);
and
3-5 - bulk MgB_2 high-pressure (2 GPa, 1 h) synthesized at 1050, 800 and 600 °C, respectively;

Introduction

Motivation

Critical current density, j_c, vs. magnetic field, $\mu_o H$, of MgB_2 materials synthesized at 2 GPa for 1 h from Mg+2B at 800 and 1050 °C;

From B (1) with grain size <5 μm, 0.66 wt% O, 0.31 wt% C, 0.48 wt% N, 0.32 wt % H

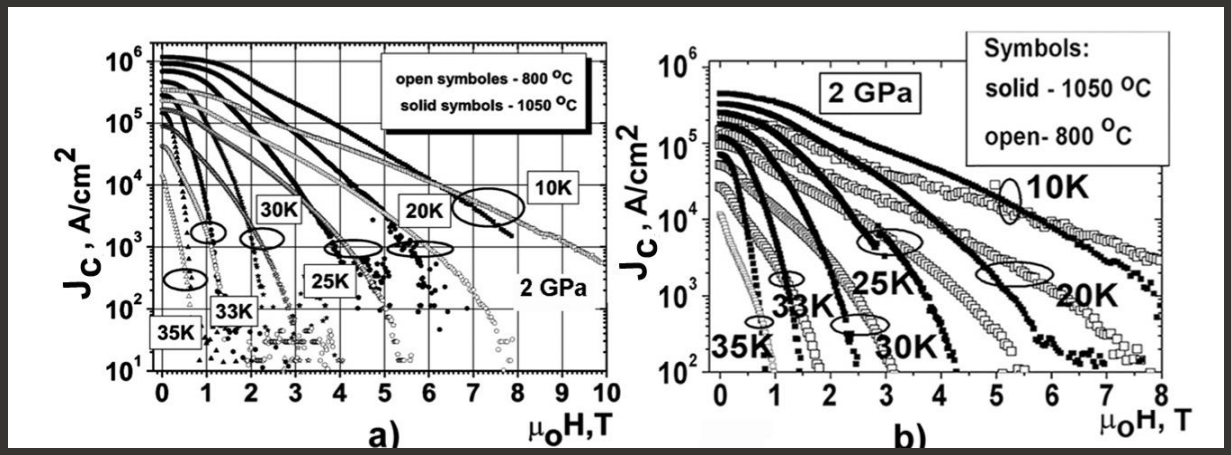

From B (2) with grain size 4 μm, 1.5 wt% O, 0.47 wt% C, 0.40 wt% N, 0.37 wt% H

j_c(0-1 T, 20 K)=0.9 – 0.7 MA/cm^2 j_c(0-1 T, 20 K)=0.4-0.3 MA/cm^2

From B(1) with 10 wt% SiC

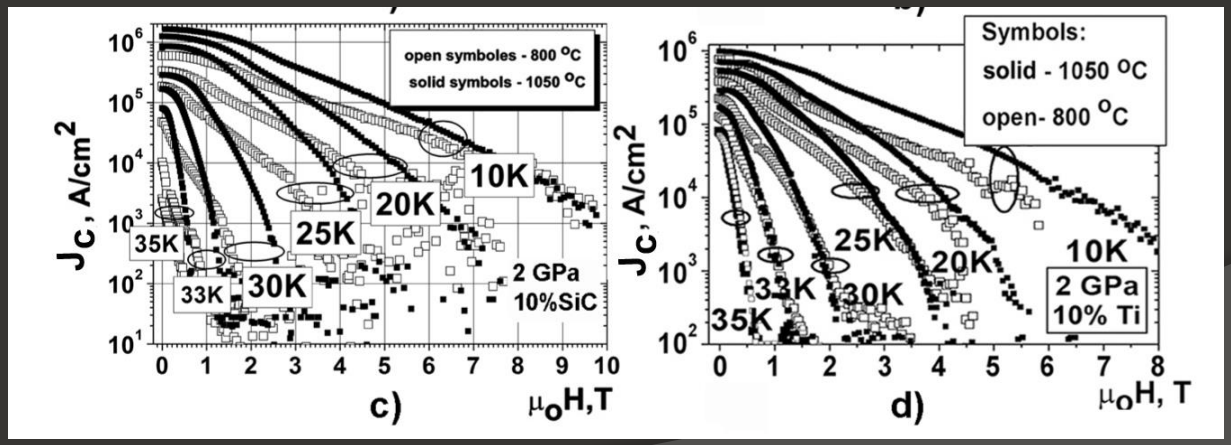

From B(2) with 10 wt% Ti

j_c(0-1 T, 20 K)=1.2 – 1.0 MA/cm^2 j_c(0-1 T, 20 K)=0.7-0.5 MA/cm^2

Introduction

B_{c2} (22 K)=15 T (No 1) and extrapolated B_{c2}(0 K)=42.1 T, as well, as irreversibility fields: B_{irr}(18.5 K)=15 T and B_{irr}(0 K)=32.5 T

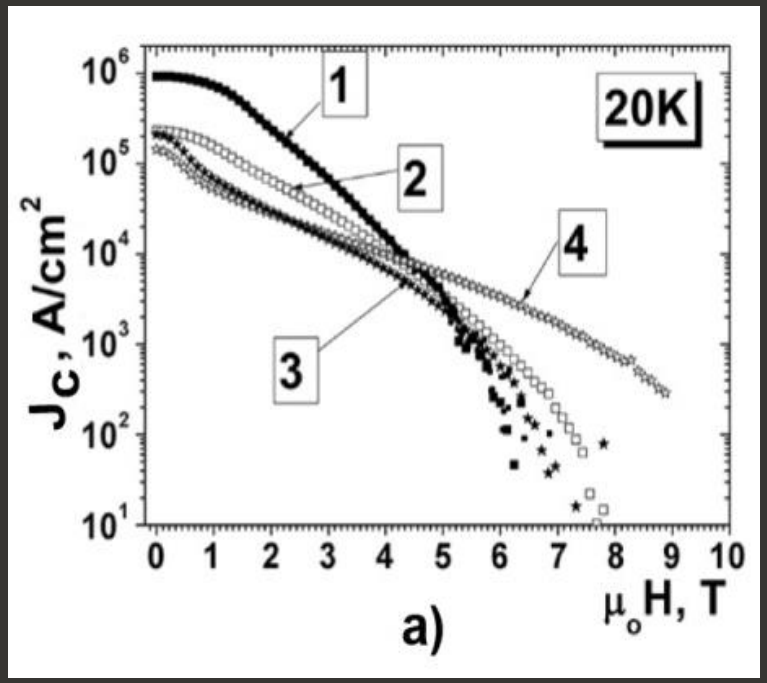

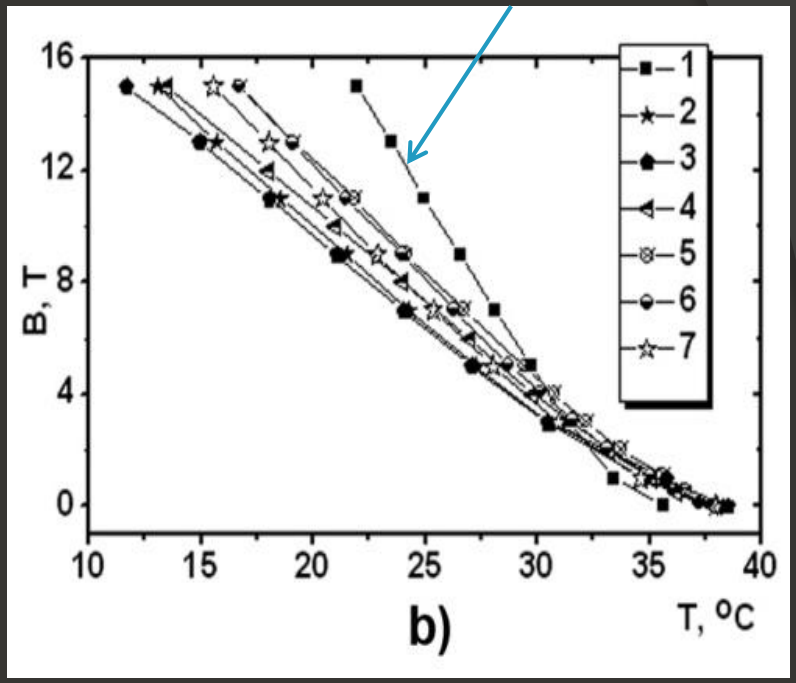

(a) Comparison of J_c at 20 K in bulk MgB_2 prepared under various temperatures at 2 GPa:
1, 2: samples made of B(I) at 1050 °C, (k=0.43) and 800 °C, (k=0.37), respectively;
3, 4 of B(II) at 800 °C and 600 °C, (k=0.32), respectively.

(b) B_{c2} of bulk MgB_2 prepared from Mg:2B :
1:B(II) at 2 GPa, 600 °C, 1 h, (HP);
2:B(III) at 30 MPa, 800 °C, 2h, (HotP);
3: B(III) at 50 MPa, 600-1050 °C, 1 h, (SPS);
4: B(III) at 2 GPa, 900 °C, 1 h (HP);
5:B(V)+10 wt.% Zr at 2 GPa, 800 °C, 1 h (HP);
6:B(V)+10 wt.% Ti at 2 GPa, 800 °C, 1 h (HP);
7:B(I)+10 wt.% SiC at 2 GPa, 1050 °C, 1 h (HP).

Structural transformations in bulk MgB_2 with manufacturing temperature increase from 800 to 1050 °C (under 2 GPa)

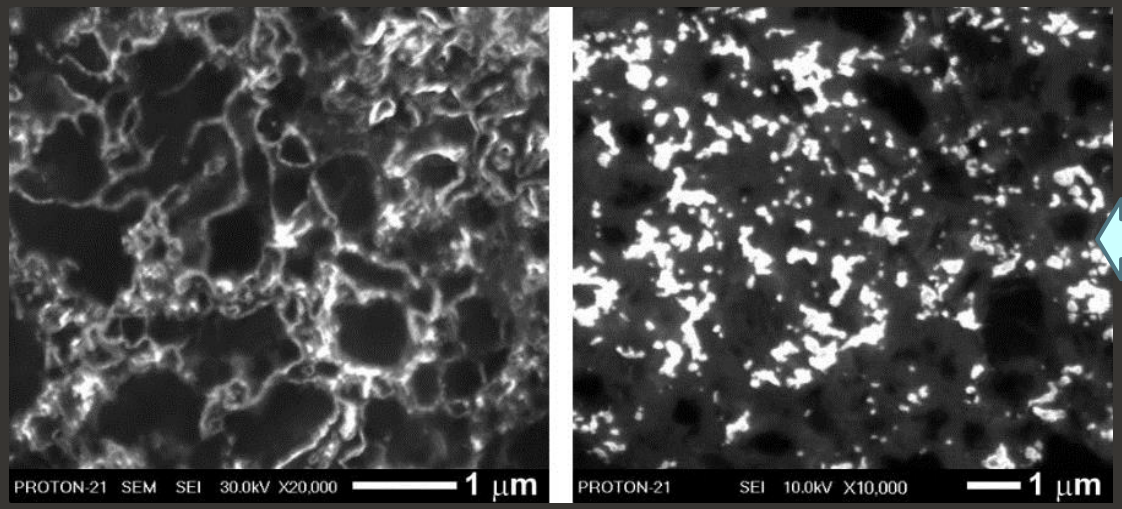

2 GPa, 800 °C, 1 h 2 GPa, 1050 °C, 1 h

99% dense MgB_2

j_c(0-1 T, 20 K) = 0.4-0.3 MA/cm^2

up to 80% connectivity

up to 94% of shielding fraction

As Auger analysis shown

- material matrix (for the sample synthesized at 2GPa 1050 °C) showed near $MgB_{2.2-1.7}O_{0.4-0.6}$ stoichiometry as a result of multiple analyzing after multiple etching steps (providing depth profile)

-bright Mg-B-O nanolayers (10-20 nm) had near $MgB_{1.2-2.7}O_{1.8-2.5}$ stoichiometry

-separate bright Mg-B-O inclusions had near $MgB_{0.6-0.8}O_{0.8-0.9}$ stoichiometry

-higher magnesium borides MgB_x which appear the most black have near $MgB_{11-13}O_{0.2-0.3}$ stoichiometry

The size and amount of higher magnesium borides (black inclusions with near $MgB_{11-13}O_{0.2-0.3}$ stoichiometry according to Auger study) decreasing with manufacturing temperature increase

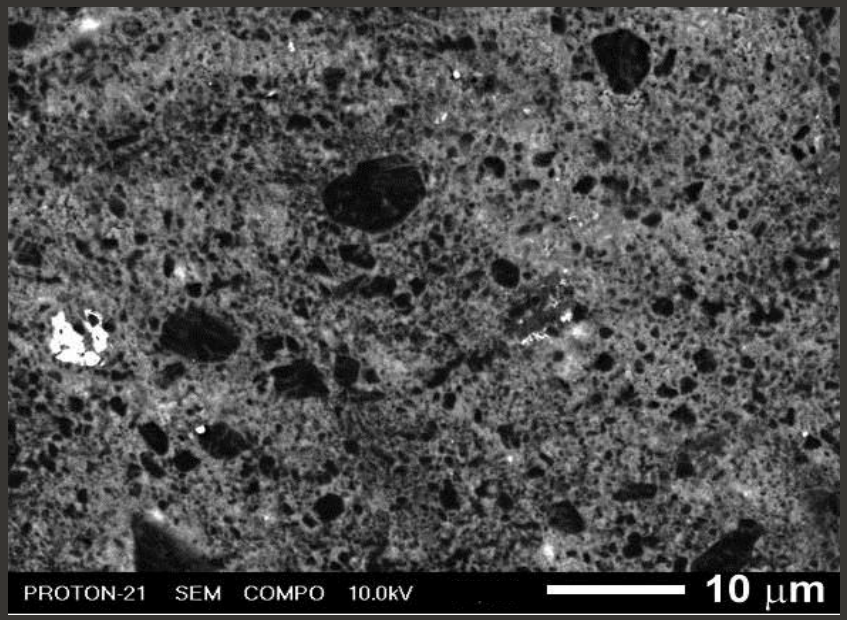

Mg:2B, 2 GPa, 800 °C, 1 h

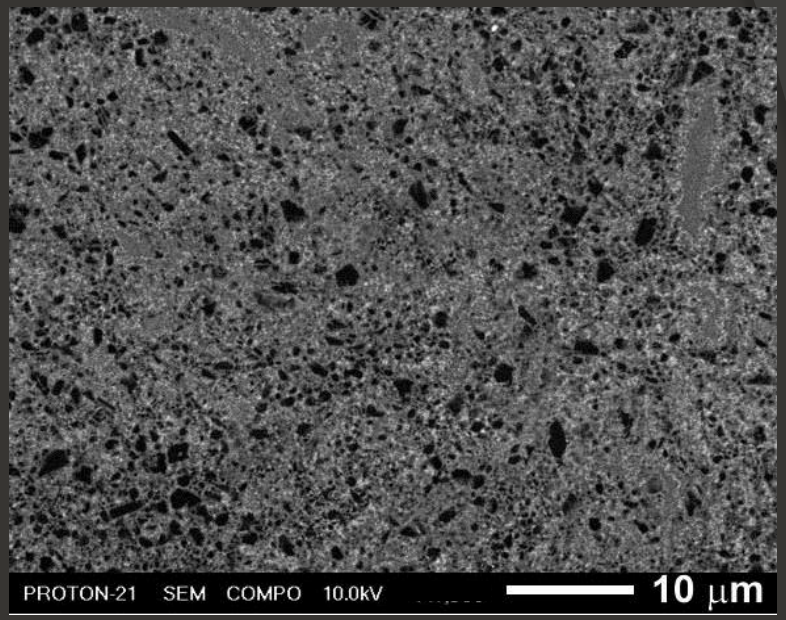

Mg:2B, 2 GPa, 1050 °C, 1 h

The Berkovich nanohardnes and Young modulus of such inclusions as estimated under the 10-60 mn-load were 32.2±1.7 and 385±14 GPa, respectively, what were even higher than that for sapphire: 31.1±2.0 and 416±22 GPa.

Density of states (DOS)

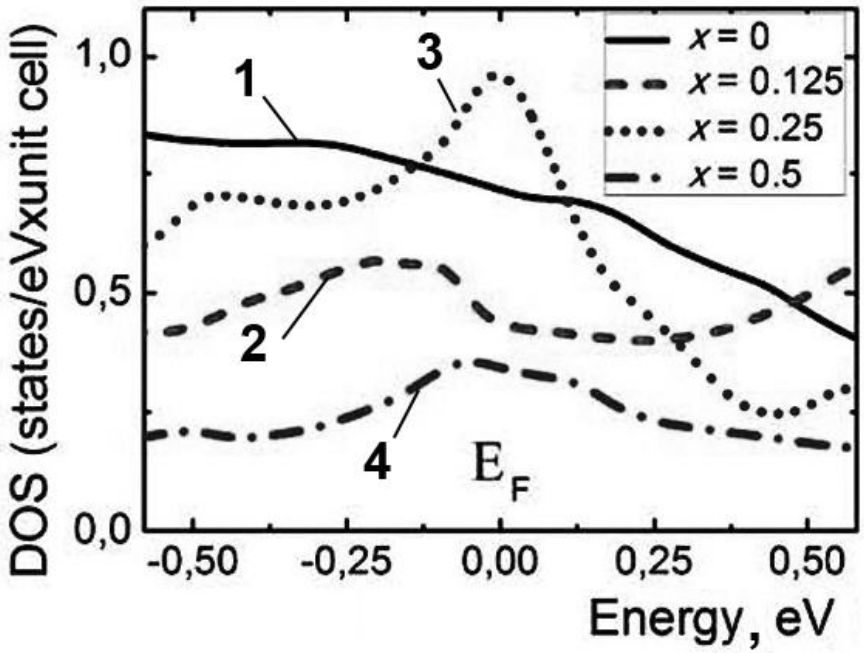

Calculated density of states (DOS) for MgB_2 (1) and $Mg(B_{1-x}O_x)_2$: $MgB_{1.75}O_{0.25}$ (2), $MgB_{1.5}O_{0.5}$ (3) MgBO (4).

We have applied the density functional theory [1] based on a full-potential linearized augmented plane wave method with the generalized gradient correction to exchange-correlation potential [2] (the program package WIEN2k [3]). In the nearest vicinity of the Fermi energy E_F corresponding dependencies are not constant and their changes with x are non-monotonous. But, in any case, all studied compounds are conductors with a non-zero density of states at the Fermi level. Large density of delocalized states proves the metallic type of the charge transport in them.

[1] Parr R G and Yang W 1989 Density-Functional Theory of Atoms and Molecules, *Oxford Univ. Press*.
[2] Perdew J P, Burke S and Ernzerhof M Phys. 1996 *Rev. Lett.* 77 3865
[3] Blaha P, Schwarz K, Madsen G K H, Kvasnicka D and Luitz J 2001 WIEN2K, An augmented plane wave + local orbitals program for calculating crystal properties. *Techn. Univ. Wien*.

The highest DOS was observed in the case of $MgB_{1.5}O_{0.5}$ (which was even higher than that for MgB_2) and according to Auger estimation the superconducting matrix demonstrated near $MgB_{2.2\text{-}1.7}O_{0.4\text{-}0.6}$ stoichiometry.

Estimation of the type of pinning

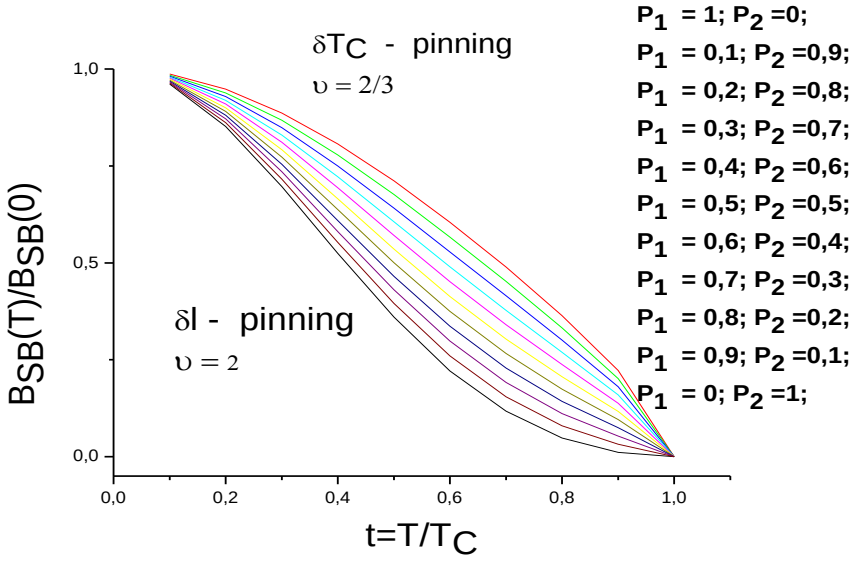

Dependences $B_{SB}(T)$

$$B_{SB}(T) = P_1 B_{SB}^{T_C} + P_2 B_{SB}^{l}$$

P_1 - δ-T_C; P_2 - δ-l

The work [G.Blatter, et.al, *Reviews of Modern Physics* 1994, v. 66, No. 4, p.p. 1125 – 1380] considers the models of Abrikosov vortexes behavior in HTS and the following types of their pining: δ-T_C pinning (in the areas of fluctuation of critical temperature, T_C) and δ-l pinning (in the areas of fluctuation of free path length, l), their combinations. The partial input of δ-T_C and δ-l into collective pinning was estimated based on the determination of temperature dependence $B_{SB}(T)$ from $J_C(B)$ temperature dependences using equatio$B_{SB}(T) = P_1 B_{SB}^{T_C} + P_2 B_{SB}^{l}$, where B_{SB} is the field in which replacement of single vortex pinning for pinning of small vortex bundle takes place.

Temperature dependences of transitions between single vortex pinning and small vortex bundle pinning

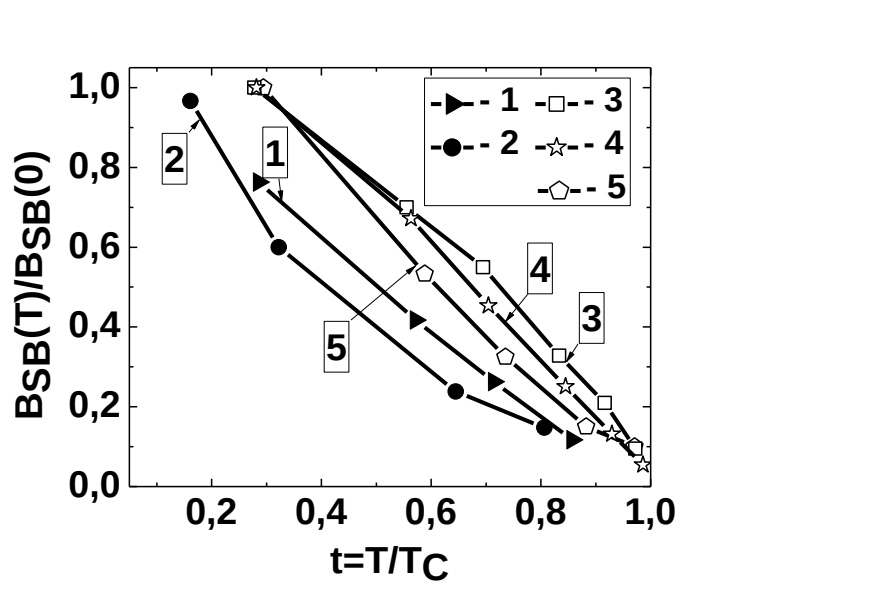

The estimated contributions in pinning were:

1- P_1=0.5, P_2=0.5;
2 - P_1=0,2; P_2=0.8;
3 - P_1=0.7, P_2=0.3;
4 - P_1=0.6, P_2=0.4;
5 - P_1=0.4; P_2=0.6

(P_1 - δ-T_C; P_2 - δ-*l*)

1 – film as deposited in Ar from MgB_2 target (Type 1),
2 – the same film after repeated annealing in vacuum (Type 3);
and
3-5 - bulk MgB_2 high-pressure (2 GPa, 1 h) synthesized at 1050, 800 and 600 °C, respectively;

It has been shown that for attaining maximal Jc in low and medium magnetic fields in bulk MgB_2 the most effective is δ-T_C pinning or combined δ-T_C (dominant) with δ-l. For attaining high Jc in high magnetic fields the δ-l pinning should be prevailed in bulk MgB_2. For nanocrystalline oxygen-containing films the increase of Jc in low and high magnetic fields correlates with increase of δ-T_C pinning contribution. Films with combined type of pinning with equal partial contributions of δ-T_C and δ-l (P_1 =P_2 =0.5) demonstrate the J_C(0 T) =1.8×10^7 A/cm^2 and J_C(5 T)=2×10^6 A/cm^2 at 10 K.

High-pressure (2 GPa, 800 °C, 1 h) treated wire from MgB_2

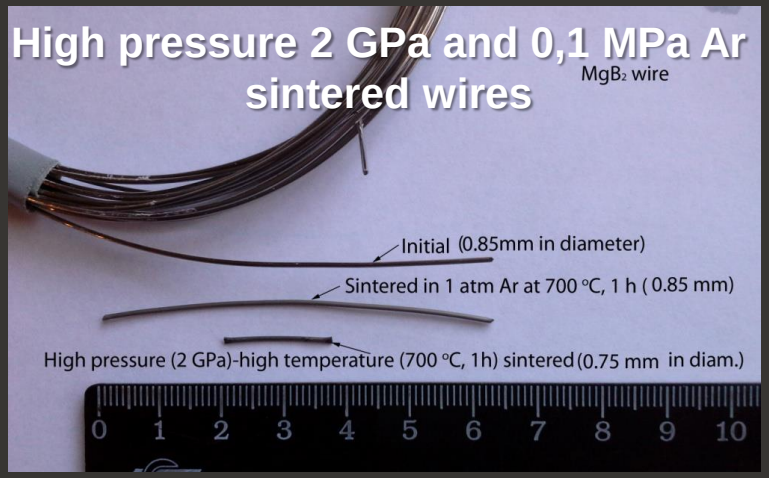

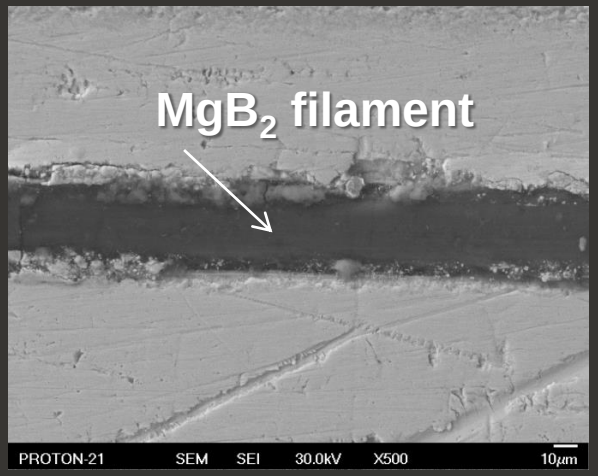

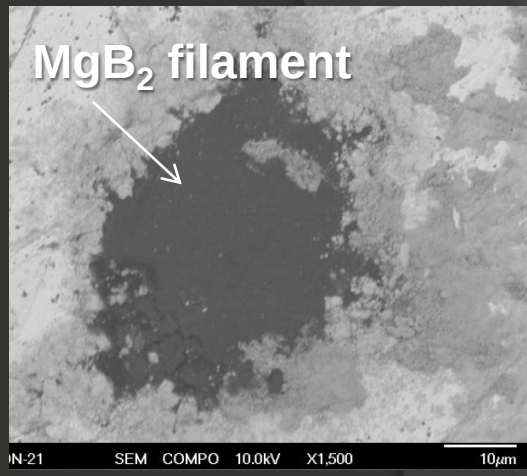

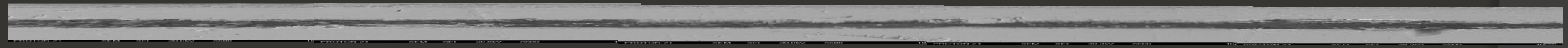

Panorama of MgB_2 filament after high pressure-high temperature treatment

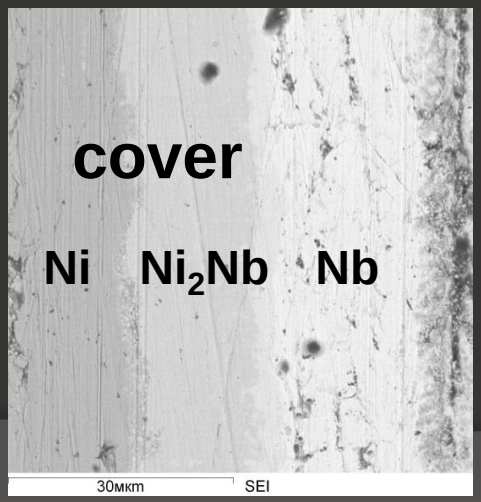

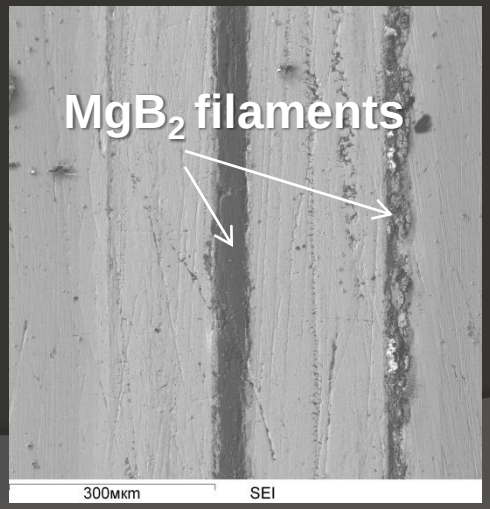

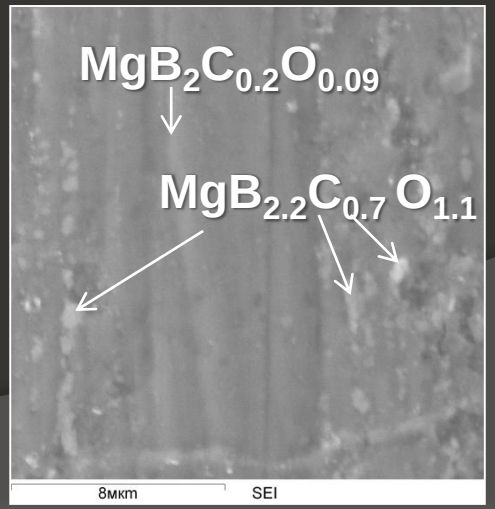

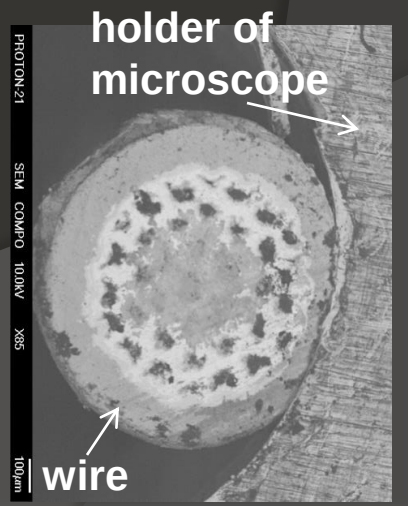

HPA cylinder-piston(V_p= 6300 cm^3) P=1-2 GPa, T =600-1100 °C, Press ASEA 140 MN effort

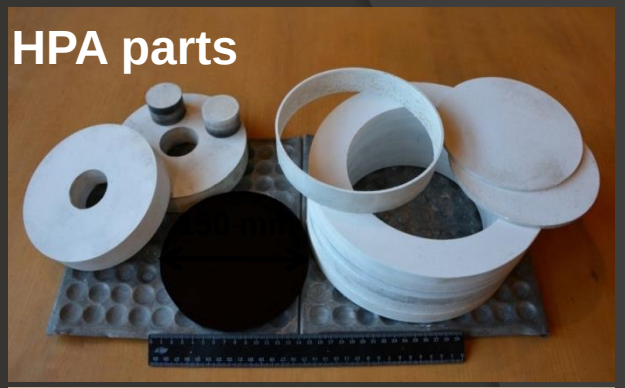

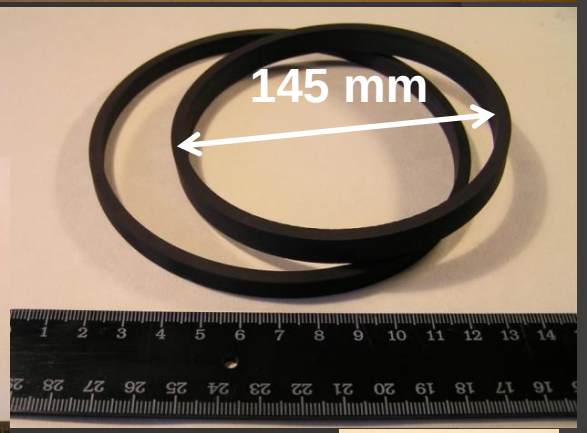

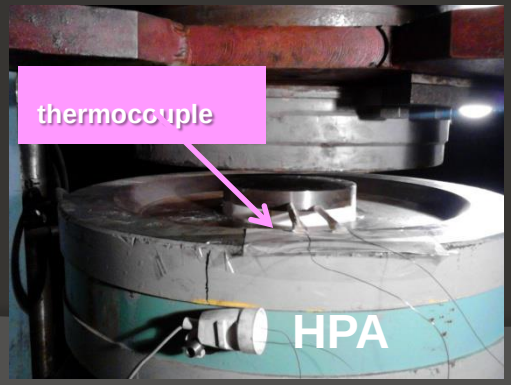

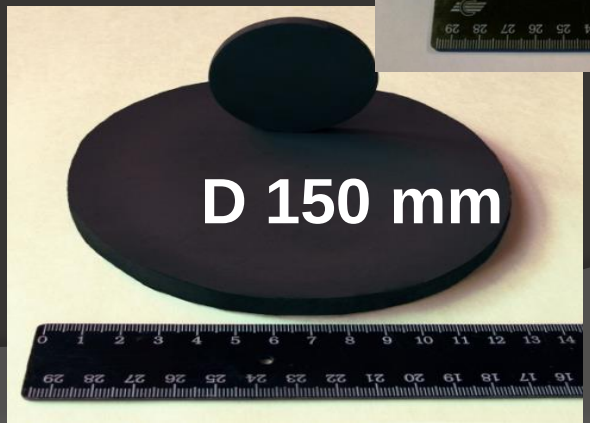

Items from MgB_2

MgB_2-based superconductors

working temperature 20-30 K

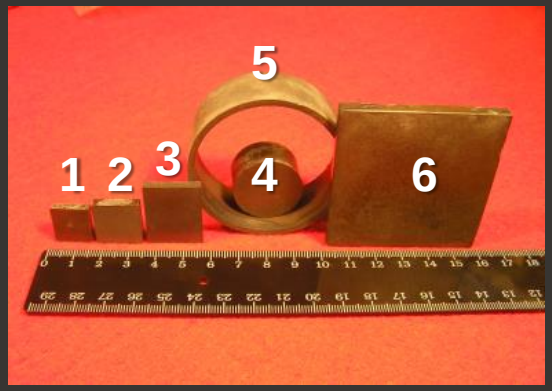

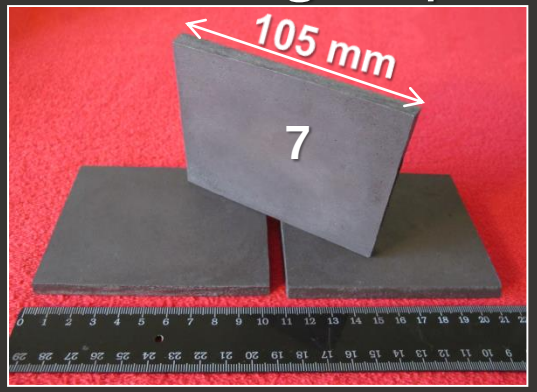

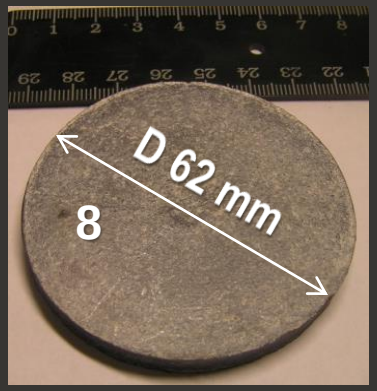

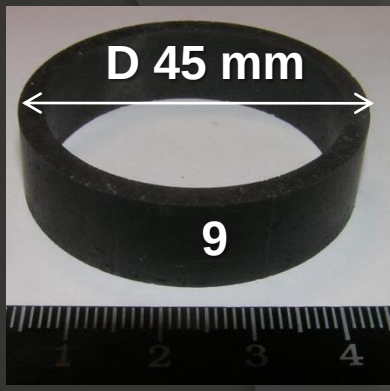

1-4, 8, 9 - High pressed (2 GPa); 5 – HIP (0.1 GPa); 7- Hot Pr. (30 MPa)

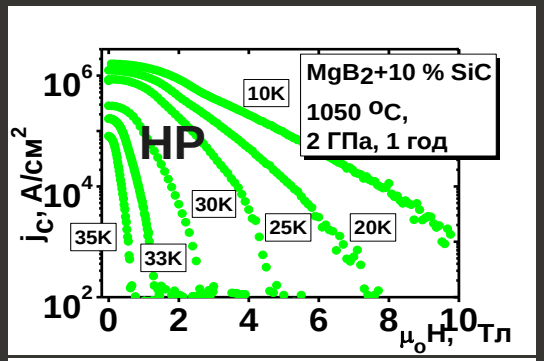

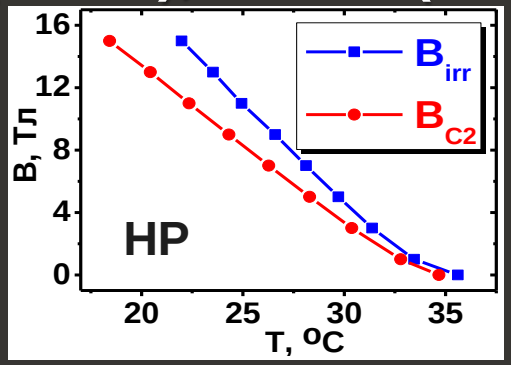

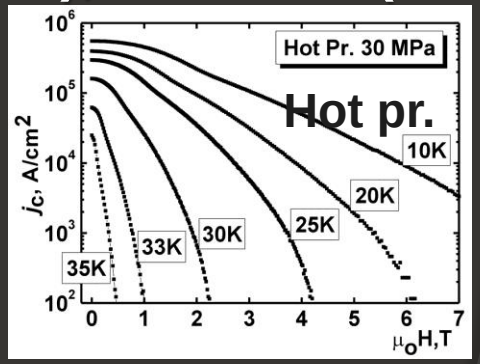

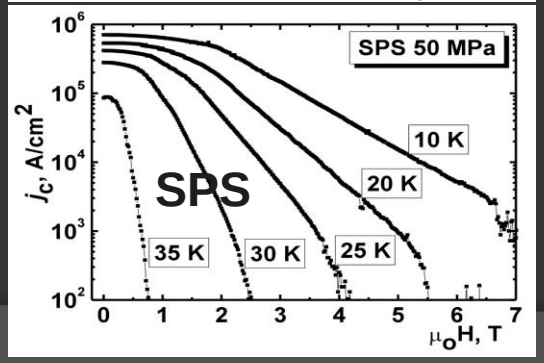

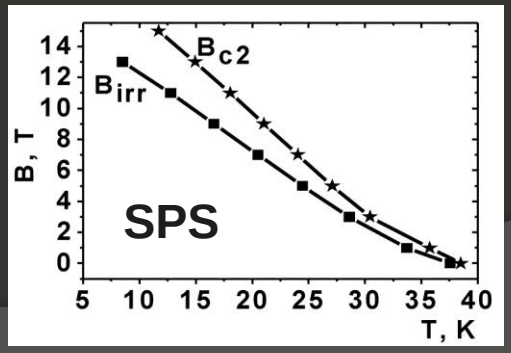

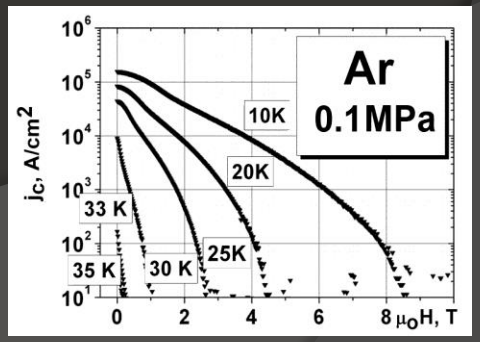

Conclusions

- The comparison of nanostructures of MgB_2 oxygen-containing thin film (with thickness of 140 nm) and highly dense oxygen-containing bulk materials demonstrating high SC performance gave us reasons to conclude that critical current density, j_c, of MgB_2 –based materials to high extend depends on distribution of admixture oxygen what can be regulated by manufacturing conditions and by synthesis temperature, in particular.

- The higher j_c of MgB_2 thin films as compared to bulk was explained by the higher density of finer oxygen-enriched Mg-B-O inhomogeneities in the film structure.

- The results of calculations of the electron density of states in MgB_2, $MgB_{1.75}O_{0.25}$, $MgB_{1.5}O_{0.5}$ and MgBO showed that all the compounds are conductors with metal-like behavior with maximum for $MgB_{1.5}O_{0.5}$ (what it is even higher than for oxygen-free MgB_2).

- The stoichiometry of the matrix of bulk MgB_2 materials having high *SC* performance was about $MgB_{2.2\text{-}1.7}O_{0.4\text{-}0.6}$ (according to Auger quantitative analysis), i.e. very near to the composition with calculated highest DOS: $MgB_{1.5}O_{0.5}$. The introduction of high amount of oxygen into MgB_2 structure cannot dramatically reduce material's T_c and allows obtaining high j_c.

- Films with combined type of pinning with equal partial contributions of δ-T_C and δ-l ($P_1 = P_2 = 0.5$) demonstrate the J_C(10K, 0 T) =1.8×10^7 A/cm^2 and j_C(10K, 5 T)=2×10^6 A/cm^2 at 10 K.

Thank you for your kind attention!

Estimation of MgB_2 density

Table 2. Characteristics (critical current density-j_c, maximal pinning force-$F_{p(max)}$, amount of MgB_2, MgO and MgB_4 estimated from Rietveld refinements, and density-ρ) of MgB_2-based materials prepared under different *P-T* conditions from Mg and B taken in MgB_2 stoichiometry or from MgB_2 powder using different methods: under high quasihydro-static pressure –HP, by hot pressing HotP, by spark plasma sintering – SPS, by pressureless sintering under 0.1 MPa of Ar – PL.

No	Preparation	Type of B	*P*, MPa	*T*, °C	j_c, MA/cm^2, at 0-1 T, at 20 K	$F_{p(max)}$/ 10^9(N/m^3) at 20 K	MgB_2/MgO/ MgB_4, wt%	Den-sity, ρ
1.	in-situ, HP	I	2000	1050	0.9 – 0.7	7.6	94/6/0	99%
2.	in-situ, HP	I	2000	800	0.2 – 0.15	1.6	91/5.5/0	98%
3.	in-situ, HP	III	2000	1050	0.4 – 0.3	2.3	87/13/0	99%
4.	in-situ, HP	III	2000	1000	0.36-0.23	2.4	86/14/0	99%
5.	in-situ, HP	III	2000	950	0.3 – 0.2	2.1	-	98%
6.	in-situ, HP	III	2000	900	0.12 – 0.06	1.1	71/13/0	98%
7.	in-situ, HP	III	2000	800	0.12 – 0.07	0.8	73/12/0	97%
8.	in-situ, HP	II	2000	600	0.14 – 0.05	0.6	64/30/0	83%
9.	in-situ, SPS	III	50	1050	0.5 – 0.4	4.6	83/4.5/12.5	94%
10.	in-situ, SPS	III	50	800	0.4 – 0.36	2.7	-	74%
11.	ex-situ, SPS	-	50	1050	0.4 – 0.3	3.3	83/6.5/10.5	96%
12.	in-situ, HotP	III	30	1050	0.08 – 0.016	0.2	46/8.5/45.5	99%
13.	in-situ, HotP	III	30	800	0.3-0.2	0.6	-	72%
14.	in-situ, PL	IV	0.1	800	0.08-0.03	1.9	90/10/0	55%
15.	in-situ, cold dens. 2 GPa, PL	III	0.1	600	0.26-0.13	1.3	94.5/5.5/0	65%

Estimation of grain sizes in MgB_2

The average crystallite sizes were calculated from line broadening in X-ray diffraction pattern by the standard program in accordance with the following:

$$\text{Crystallite size} = \frac{K \cdot \lambda}{W_{\text{size}} \cdot \cos\theta} \quad \text{with} \quad W_{\text{size}} = W_{\text{b}} - W_{\text{s}}$$

where W_{size} is the broadening caused by small crystallites; W_b is the broadened profile width; W_s is the standard profile width (0.08 °); K is the form factor; λ is the wavelength.

Table. Critical current density, j_c, vs. relative average grain size of crystallites of high-pressure sintered from MgB_2 and synthesized from Mg and B taken in1:2 ratio materials

High pressed at 2 GPa for 1 h at T_s, °C	average crystal sizes	lattice parameters		j_c, kA/cm^2 at 10 K		j_c, kA/cm^2 at 20 K	
		a (nm)	*c* (nm)	0 T	1 T	0 T	1 T
From MgB_2 (10 μm and 0.8 % of O)							
700	19.7 nm	0.30805	0.35188	-	-	-	-
800	18.8 nm	0.30822	0.35212	-	-	-	-
900	18.5 nm	0.30820	0.35208	56	14	36	8
1000	25.0 nm	0.30797	0.35200	28	8	19	5
From Mg chips and B (4 μm, 1.5 % O) mixed and milled in 1:2 ratio							
800	15.0 nm	0.30747	0.35188	245	142	138	79
900	21.0 nm	0.30819	0.35174	205	136	128	61
1000	37.0 nm	0.30808	0.35192	485	364	360	237

Estimation of connectivity, A_F

$$A_F = \frac{9\ \mu\Omega\cdot\mathrm{cm}}{\rho_{300} - \rho_{40}}$$

$$9\ \mu\Omega\cdot\mathrm{cm}$$

perfect connectivity for MgB_2

resistivity $\rho = \dfrac{V\cdot\sigma}{I\cdot\Delta l}$

$$\rho_{300} = \frac{V_{300}\cdot\sigma}{I\cdot\Delta l} \qquad \rho_{40} = \frac{V_{40}\cdot\sigma}{I\cdot\Delta l}$$

Δl - distance between voltage contacts

$\sigma = a\cdot b$ - cross-section area of the sample, $a\cdot b\cdot c$ - sample dimensions

V_{300} - arithmetic average of all V data at room temperature

V_{40} – voltage at 40 K

I =100 mA - current

ρ - by four probe method

Estimation of pinning mechanism

M. Eisterer " Calculation of the volume pinning force in MgB_2 superconductors" (PHYSICAL REVIEW B 77, 144524 2008)

Identification of the dominant pinning mechanism from the peak position of pinning volume force:

$$k = B_{peak}/B_n ;$$

$$B_{peak} - F_{p(max)}, \quad B_n - F_{p(max)}/2$$

The dominant pinning mechanism was determined from the volume pinning force j_cB according to a scaling procedure proposed by M.Eisterer , which eliminates the influence of the intrinsic anisotropy of MgB_2 on the field dependence of the volume pinning force. The field B_{peak}, where the maximum of the volume pinning force occurs, was normalized by the field B_n, at which the volume pinning force drops to half its maximum (on the high field side), instead of the upper critical field, B_{c2}, in the original approach for isotropic superconductors . For typical values for the anisotropy (4) and the percolation threshold (0.25) in bulk MgB_2 samples, the position of the peak, B_{peak}/B_n, is expected to be at 0.34 and 0.47 for grain boundary and point pinning, respectively. Changes in the anisotropy and the percolation threshold only slightly change the peak position, in particular in the realistic range of these parameters. Another advantage of this scaling approach is that B_n is easily available and no separate experiment for determining B_{c2} or any extrapolation to estimate the irreversibility (or Kramer) field is necessary to define the scaling field.

X-ray diffraction patterns of the materials prepared from Mg:2B under 2 GPa for 1 h without additions at 800 °C (a) and 1050 °C (b) and with 10 wt. % Ti at 800 °C (c) and 1050 °C (d).

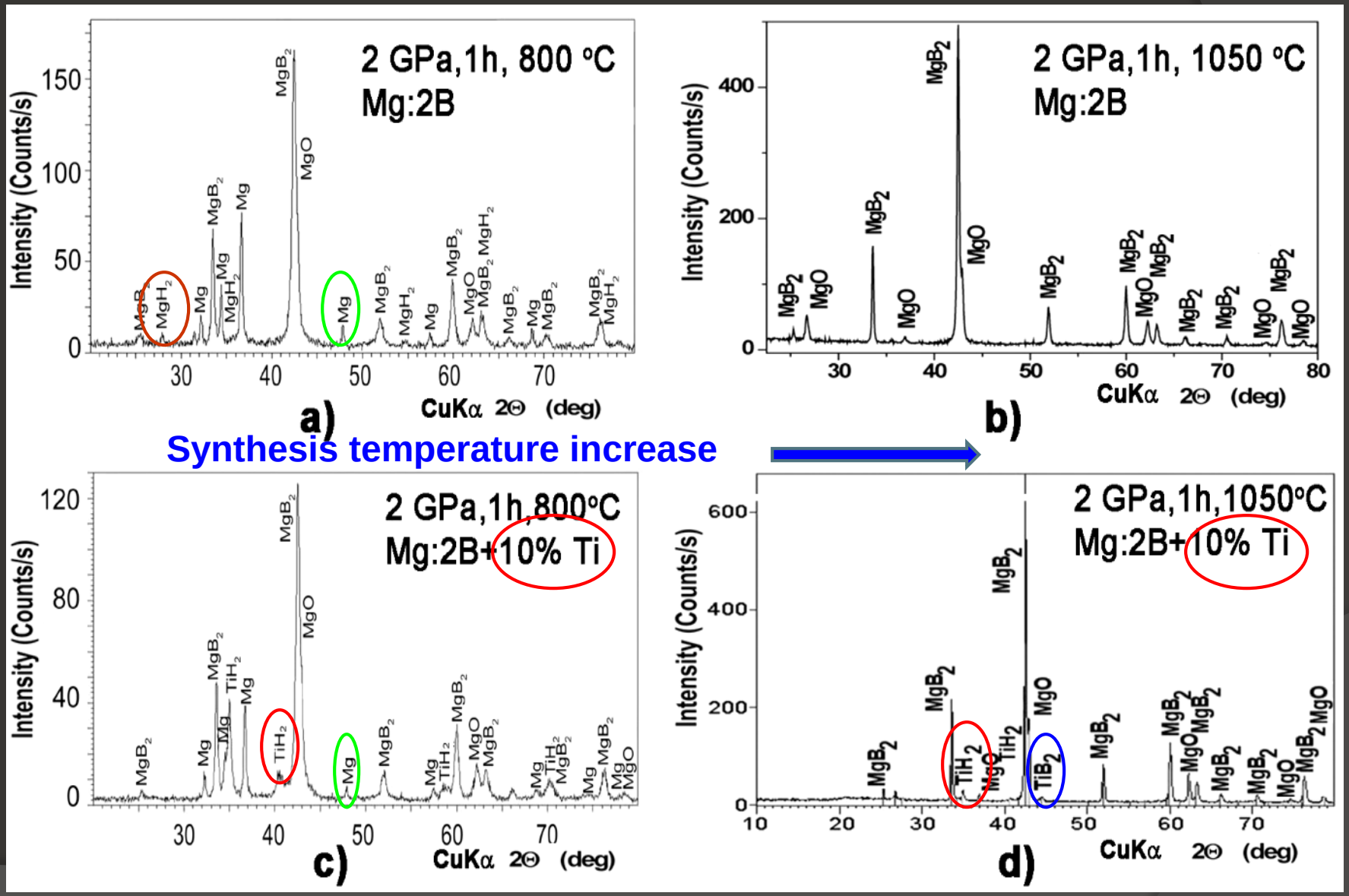

Estimation of connectivity, A_F, amount of shielding fraction, S, and type of pinning, k.

Connectivity, A_F, k-ratio: $k = B_{peak}/B_n$ and amount of shielding fraction, S, of MgB_2 materials prepared under different conditions. The numbering in tables 1 and 2 is the same.

No	Preparation	Type of B	P, MPa	T, °C	$k = B_{peak}/B_n$	A_F, %	S, %
1.	in-situ, HP	I	2000	1050	0.43	-	-
2.	in-situ, HP	I	2000	800	0.37	-	-
3.	in-situ, HP	III	2000	1050		79	94
5.	in-situ, HP	III	2000	950	-	59	81
7.	in-situ, HP	III	2000	800		57	91-100
8.	in-situ, HP	II	2000	600	0.32	18	90
9.	in-situ, SPS	III	50	1050	-	98	91
11.	ex-situ, SPS	-	30	1050	-	80	100
12.	in-situ, HotP	III	30	1050	-	32	-
13.	in-situ, HotP	III	30	800	-	73	-
15.	in-situ, cold dens. 2 GPa, PL	III	0.1	600	-	-	75
16.	in-situ, cold dens. 2 GPa, PL	III	0.1	800	-	-	84

With synthesis temperature increase the shift from grain boundary pinning towards point pinning occurs (about what k-ration increase witnessed)

CONTRADICTIONS BETWEEN X-RAY DATA AND SEM OBSERVATIONS

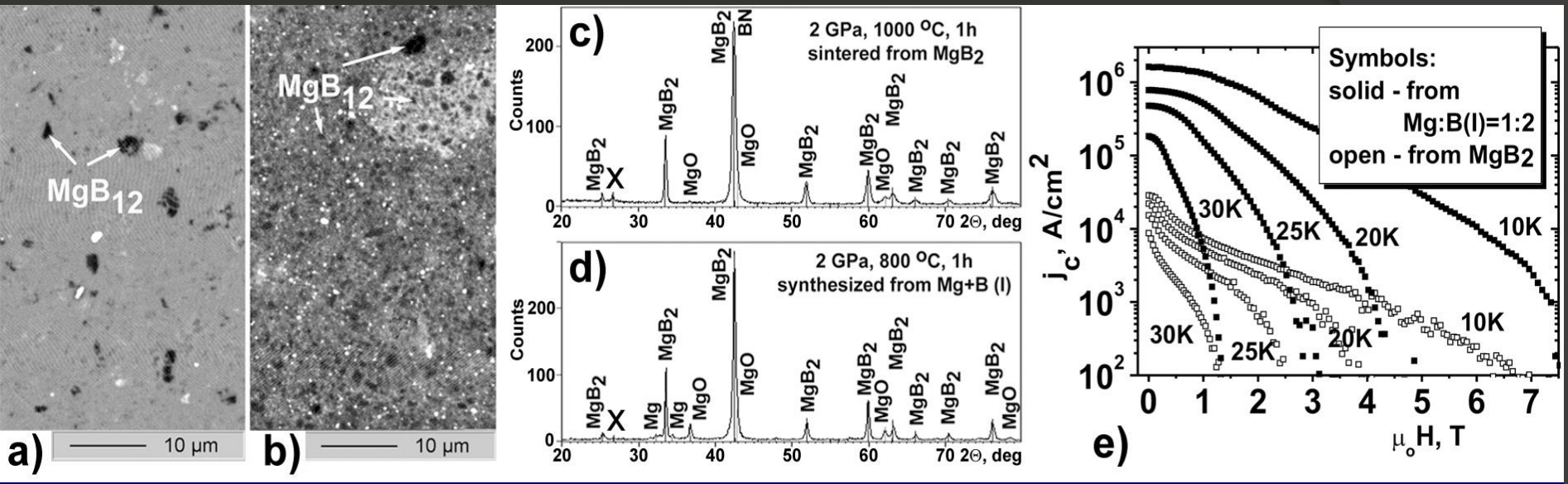

(a), (b) structures of the samples obtained by SEM in COMPOsitional contrast:
(a) sintered from MgB_2 at 2 GPa, 1000 °C, 1 h;
(b) synthesized from Mg and B taken into 1:2 ratio at 2 GPa, 800 °C, 1 h;
(c), (d) –X-ray patterns of the samples shown in Figs. 5a, b;
(e) dependences of critical current density, j_c, on magnetic fields, $\mu_o H$, at different temperatures of the samples shown in Fig. e: open symbols – sintered from MgB_2 material and solid symbols - synthesized from Mg and B taken in 1:2 ratio

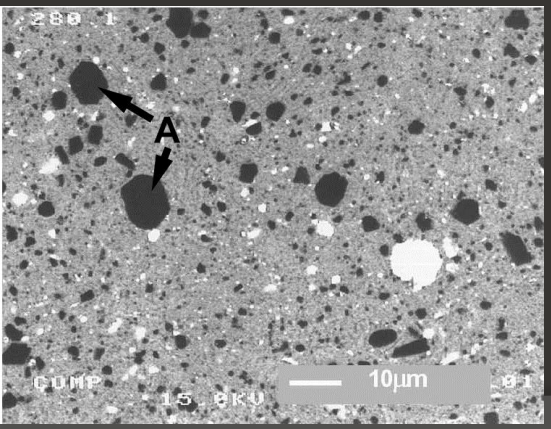

Structure of MgB_2-based material synthesized from amorphous boron and magnesium chips taken in Mg:B=1:2 ratio in contact with Ta foil at 2GPa, 800°C, 1h (BEI SEM image) shows that inclusions of black phase with near MgB_{12} stoichiometry may crystallize in hexagonal habit or have near hexagonal cross-section (see, for example, inclusion marked "A")

Each of the following non-superconducting higher magnesium borides in the Mg-B system can crystallize in the MgB_2 matrix and can influence pinning

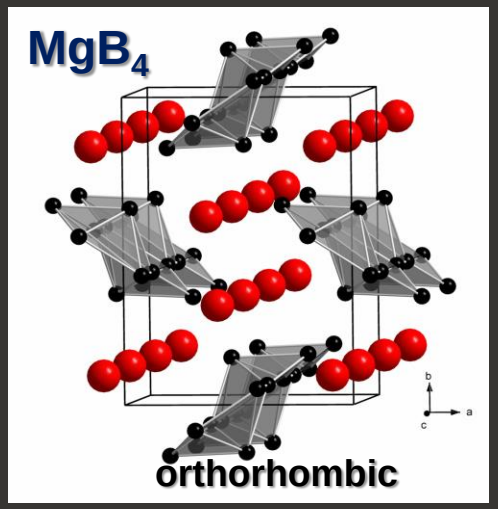

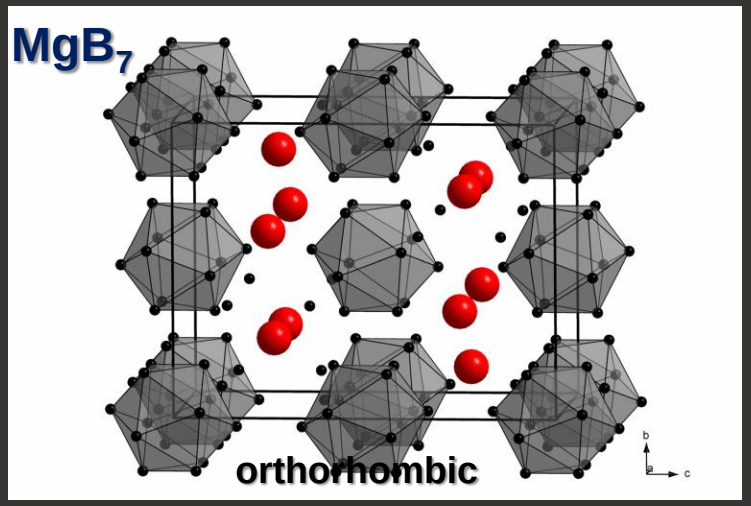

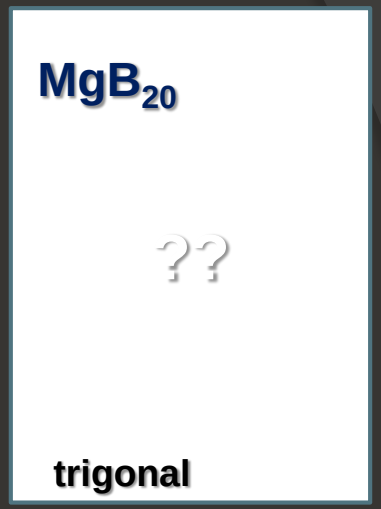

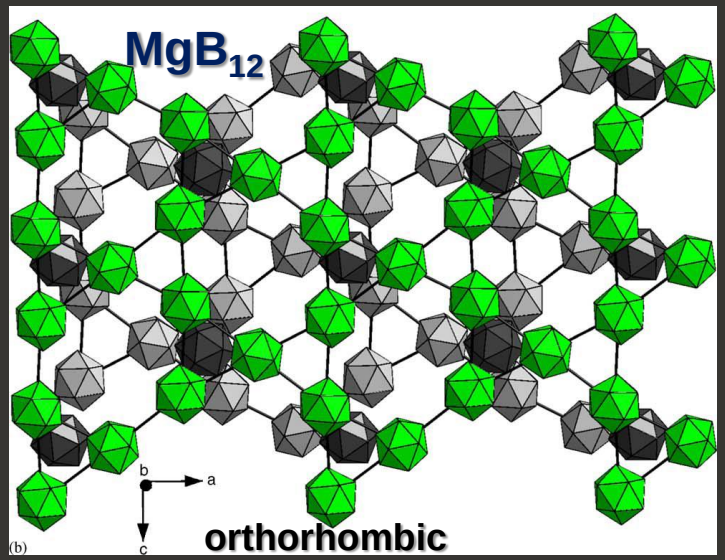

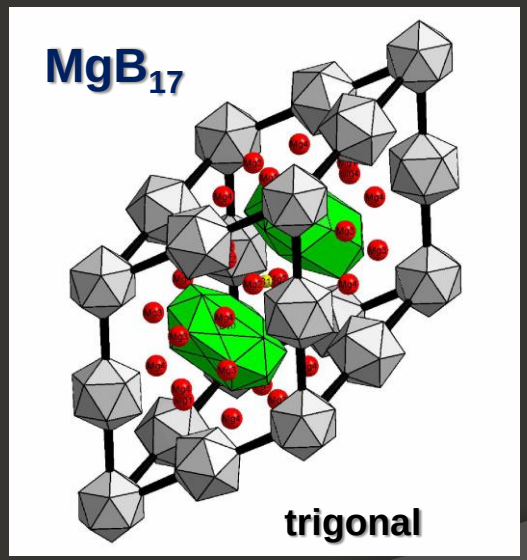

The method of preparation (pressure-temperature-time conditions) can affect the stoichiometry of the MgB_x inclusions in MgB_2. (2 GPa – MgB_{12})

Typical structures of MgB_2 prepared at 0.1 MPa – 2 GPa at low temperatures (a) - 600-800 °C and high (b) -1000-1100 °C and their compositions

0.1 MPa – 2 GPa

a)

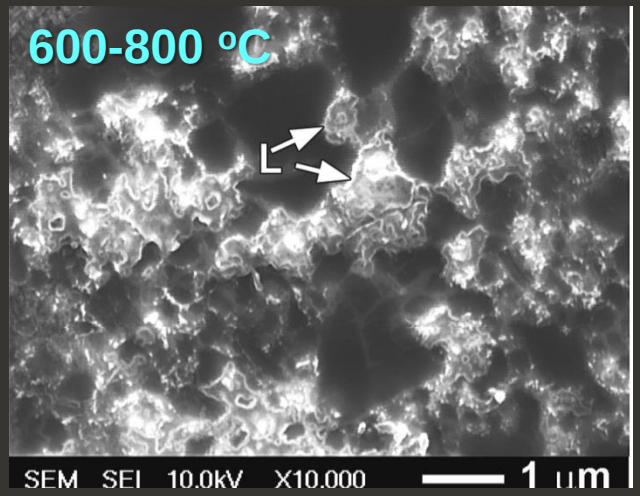

b)

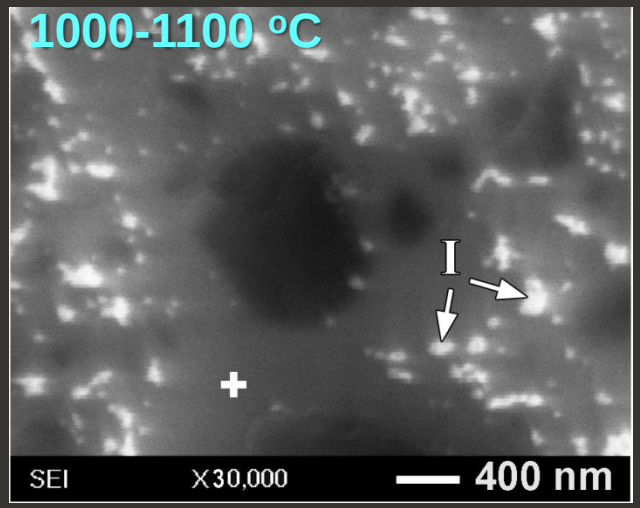

"*L* " - $MgB_{0.9\text{-}3.5}O_{1.6\text{-}2}$ white layers, thickness (15-20 nm)

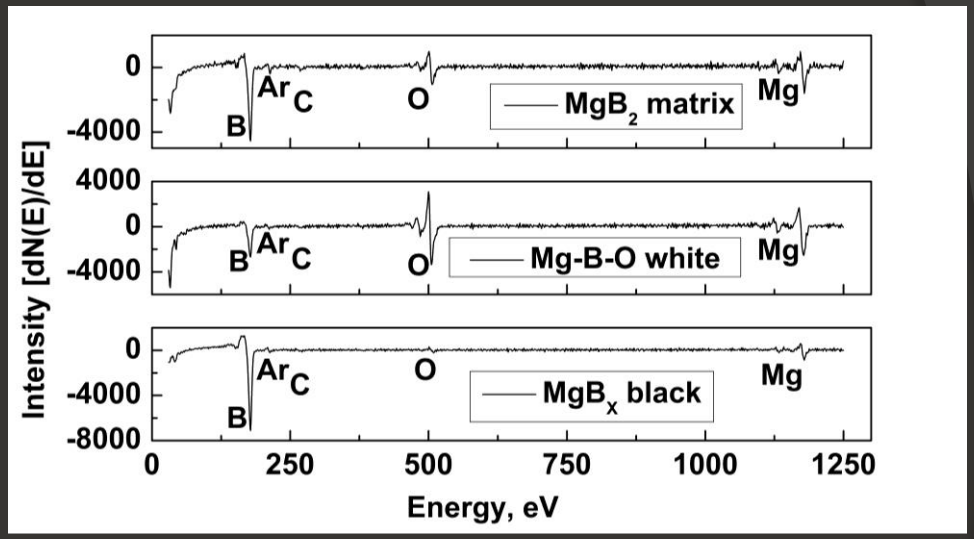

Auger spectrum

"*l*" - $MgB_{0.5\text{-}0.8}O_{0.8\text{-}0.9}$ white inclusions

$MgB_{11\text{-}13}O_{0.2\text{-}0.5}$ black inclusions

$MgB_{2.2\text{-}1.7}O_{0.3\text{-}0.6}$ gray matrix.

Auger study by JAMP−9500F

Zone of excitation being 10 nm in diameter and two lattice parameters in depth etching in Ar allows to exclude analyzing of oxidized layer on the surface!

Auger study by JAMP−9500F

zone of excitation being 10 nm in diameter and two lattice parameters in depth

Mg(I):2B(III), 1200 °C, 2 GPa, 1h

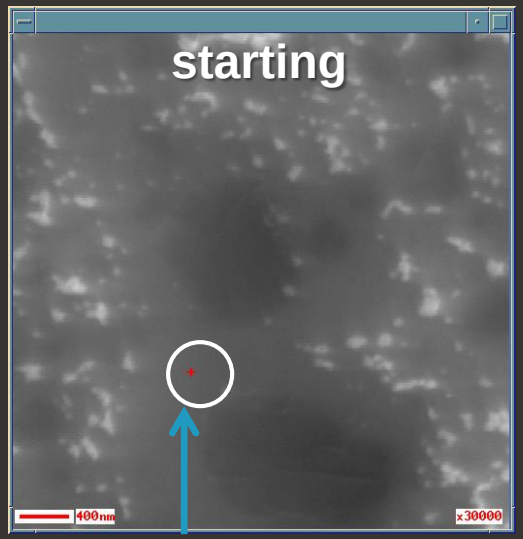

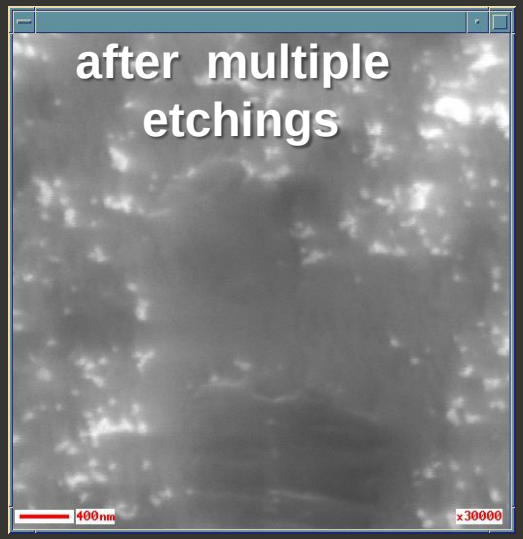

Place of analysis

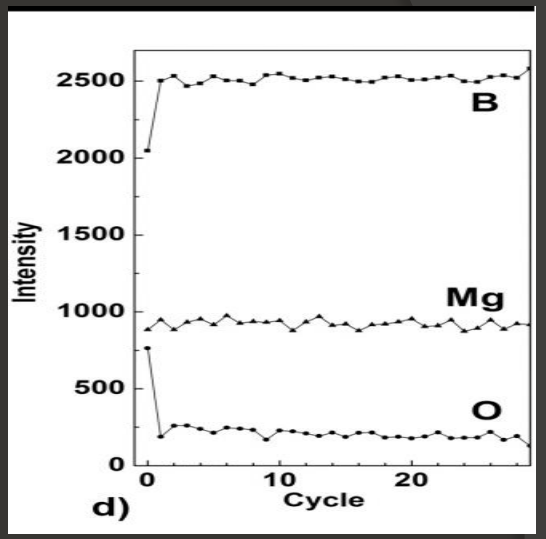

$MgB_{0.5\text{-}0.8}O_{0.8\text{-}0.9}$ white inclusions
$MgB_{11\text{-}13}O_{0.2\text{-}0.5}$ black inclusions
$MgB_{2.2\text{-}1.7}O_{0.3\text{-}0.6}$ gray matrix.

Spectrums of gray matrix

Depth profile of gray matrix

Comparing these results with that of X-ray structure analysis we can conclude that **boron incorporated into the MgB_2 structure.**
Repeated etching in Ar (in the JAMP−9500F chamber during study) and quantitative Auger analysis showed practically the same oxygen concentration in MgB_2 matrix of the structure after 30 cycles, which points to the **oxygen incorporation into the MgB_2 lattice.**

Increase of j_c in low and medium magnetic fields with increase of manufacturing temperature and effect of Ti addition

2 GPa, 1 h

from Mg:2B

from Mg:2B + 10% Ti

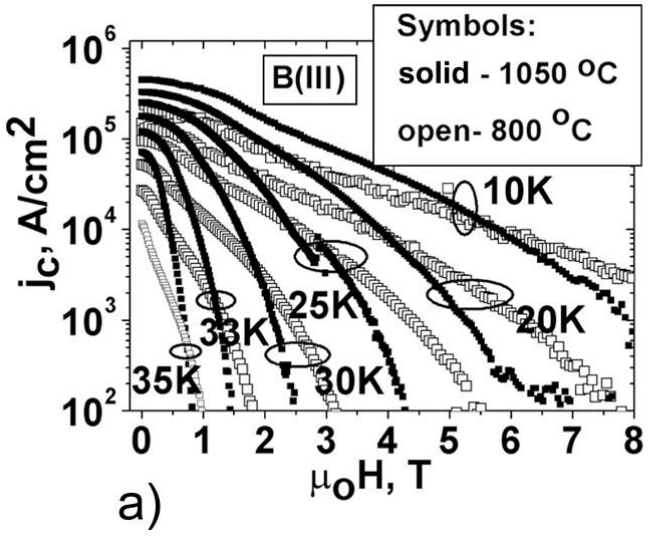

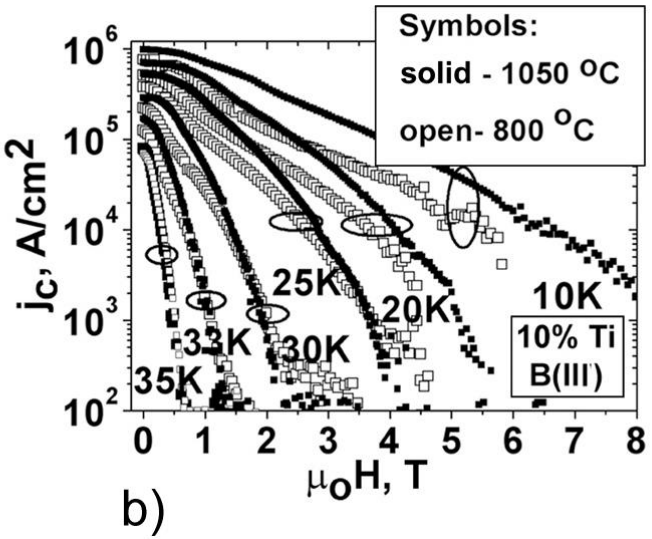

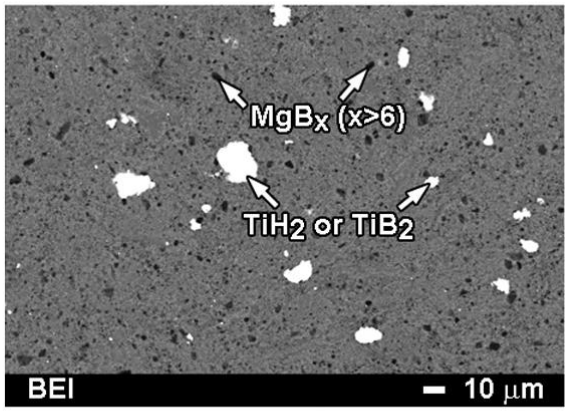

Boron amorphous: grain size 4 μm, 1.5 wt% O, 0.47 wt% C, 0.40 wt% N, 0.37 wt% H

- The critical current density of MgB_2 – based materials usually increases at low and medium magnetic fields with increasing manufacturing temperature, but lower manufacturing temperatures can result in a j_c increase at high magnetic fields.
- A shift from grain boundary pinning to point pinning was observed
- A positive effect in enhancing the critical currents of MgB_2 is played,, by dopants, such as Ti, for example.

MgB_2 for fault current limiter

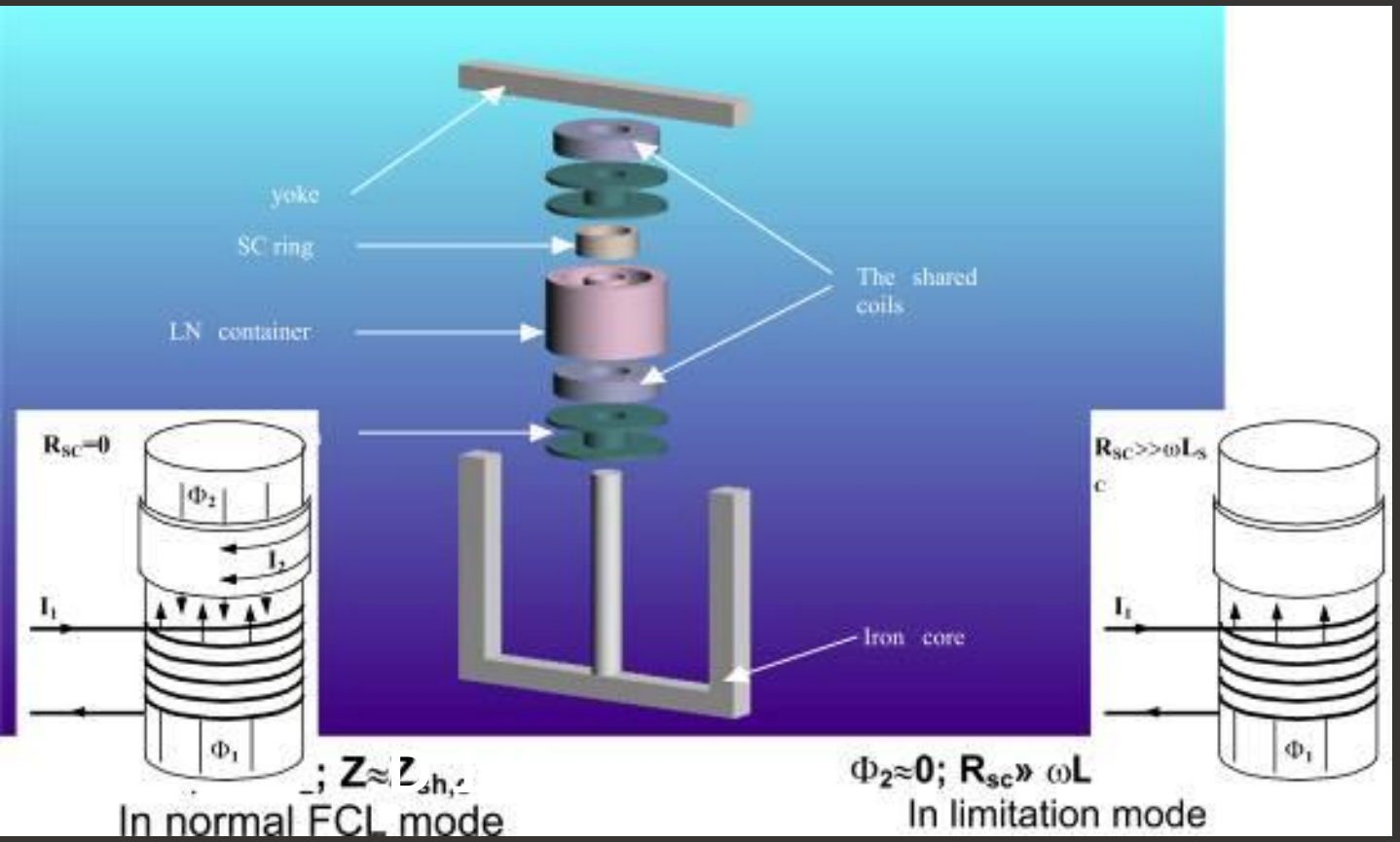

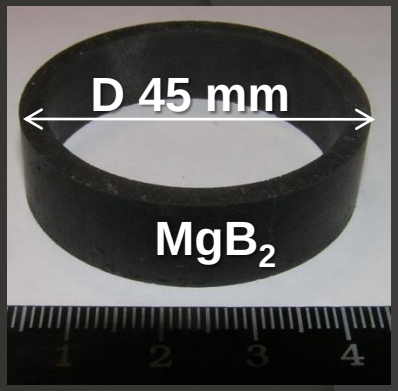

Rings cut from MgB_2 blocks

Transformer- type fault current limiter (Budapest University of Technology and Economics)

At fault event an increase in the circuit current causes a growth of the current in a superconductor higher than the critical value. The SC-or passes into the resistive state introducing a required for limitation impedance in the circuit (2–4 ms and 1 ms) .

Smart application of HP and hot-pressed MgB_2-based materials

Characteristics of the MgB2-based material synthesized at 30 MPa, 800 °C, 2 h from amorphous boron (III) (H.C. Starck, 1.5 % O, 4 μm grains) and magnesium (I) taken in the MgB_2 stoichiometry and of the ring cut from this material:

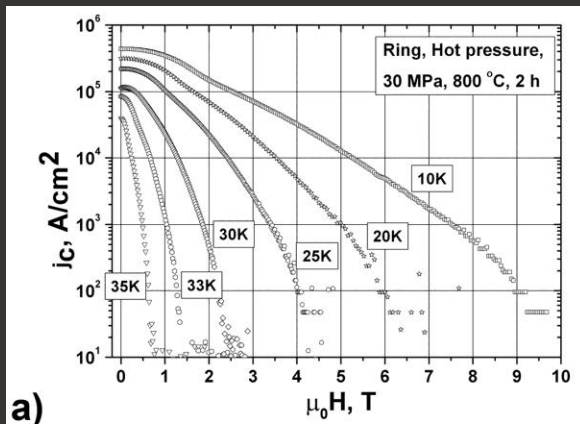

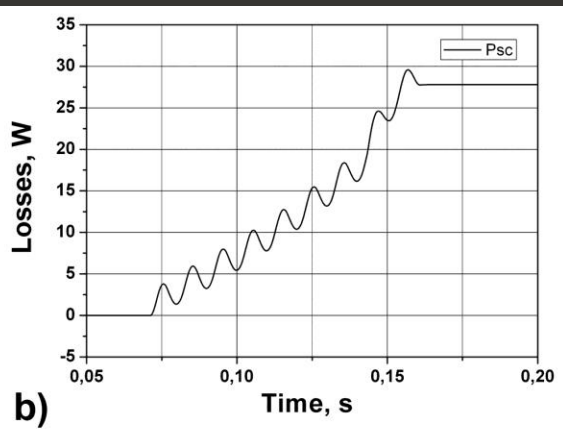

Quenching current 24000 A.

j_c= 63200 A/cm².

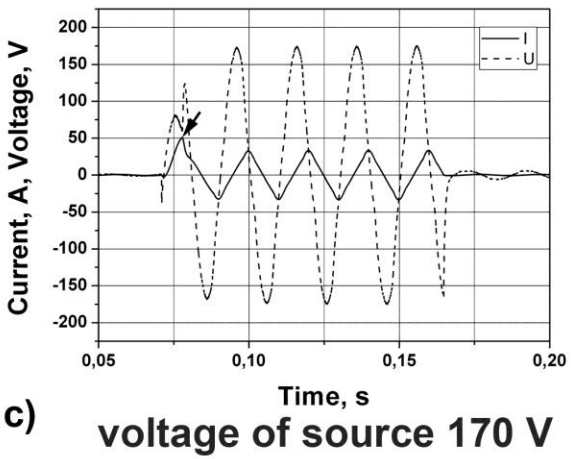

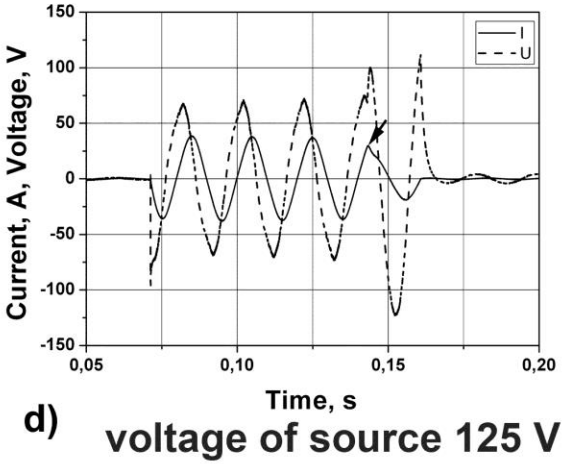

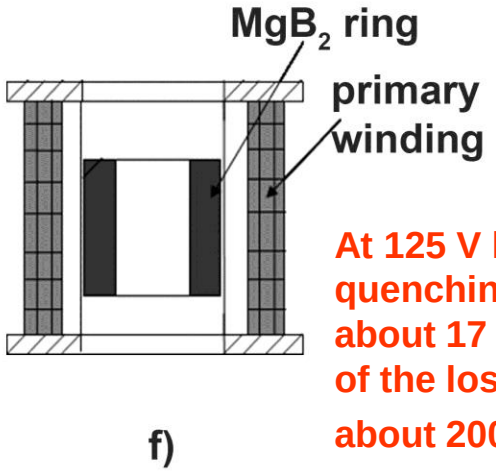

At 125 V losses till quenching are about 17 J. Power of the losses is about 200 W.

Typical oscilloscope traces of the current (solid lines) and voltage drop across the primary normal-metal winding (dashed lines) at 4.2 K. Arrows show the quenching current. Voltage of source was 170 V (c) and 125 V (d);
e) ring: outer diameter – 45 mm, height - 11.6 mm, wall thickness – 3.3 mm.

First MgB2-based 1.3 kW motor by MAI (Moscow) , IPHT (Jena), ISM NASU, Kiev

Experimental HTS Motor for 20 K Temperature

Cross-section of HTS Motor

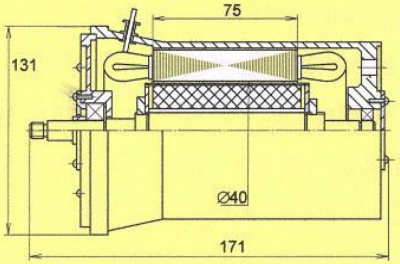

General View of HTS Motor

Compound HTS-Ferromagnetic Rotor With YBCO Bulk Elements

General View of YBCO Samples

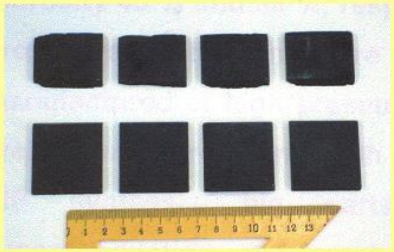

Rotor With YBCO Bulks

Compound HTS-Ferromagnetic Rotor With MgB_2 Bulk Elements

General View of MgB_2 Bulk Samples

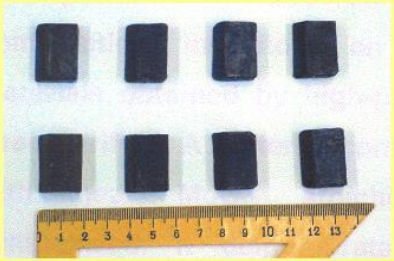

Rotor With MgB_2 Samples

Test results of reluctance motor with MgB_2 blocks

Temperature: T = 15 … 20 K

Phase voltage: U = 120 V

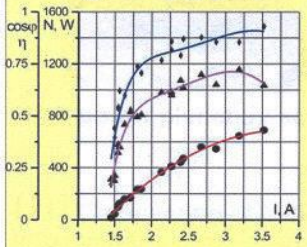

Phase voltage: U = 160 V

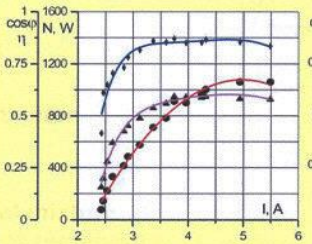

Phase voltage: U = 210 V

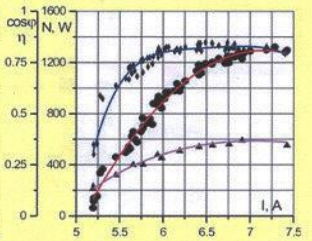

◆ - efficiency, ● - output power, ▲ - power factor

Test results of reluctance motor with YBCO blocks

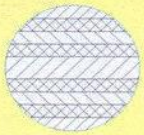

Temperature: T = 15 … 20 K

Phase voltage: U = 120 V

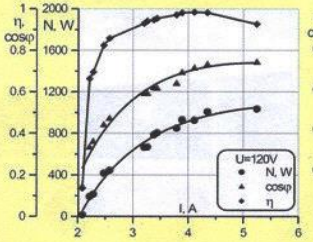

Phase voltage: U = 160 V

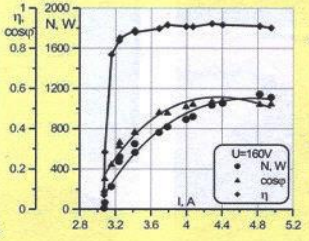

Phase voltage: U = 215 V

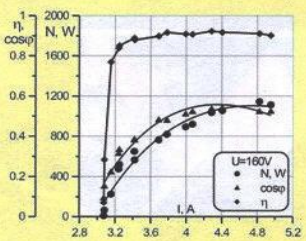

◆ - efficiency, ● - output power, ▲ - power factor

Conclusions

- The distribution of nanostructural inhomogeneities, such as areas with a high concentration of B and impurity O, plays a key role in the variation of j_c in MgB_2 materials.
- Auger and SEM studies show that with increasing manufacturing temperature oxygen enriched 15-20 nm thick nano-layers transform into distinct dispersed Mg-B-O inclusions.
- In parallel, the Ti addition results in a further increase in j_c , because Ti fosters the localization (or segregation) of oxygen and of higher magnesium borides and facilitates the formation of a homogeneous MgB_2 matrix with low oxygen content, but with Mg-B-O and MgB_x pinning centers.
- At low synthesis temperature Ti can absorb hydrogen forming titanium hydrides, thus preventing the formation of MgH_2 and promoting the material densification.
- The positive effect of Ti addition results from the high ability of Ti to absorb H, O, and Mg.

Experimental

2 GPa - HP, 30 MPa- HotP, 50 MPa – SPS, 0.1 MPa Ar - PL

Initial materials

(I) *in-situ* from Mg:B=1:2 (MgB_2) , from Mg:B=1:7 and 1:12 mixing and milling in a high speed activator for 3-5 min

- ✓ Boron (B) amorphous

Characteristics of initial boron powders.

Type of B	Grain size	O, wt%	C, wt%	N, wt%	H, wt%
I	<5 μm	0.66	0.31	0.48	0.32
II	<1 μm	-	3.5	1.02	0.87
III	4 μm	1.5	0.47	0.40	0.37

- ✓ Magnesium (Mg)

  Mg(I) turning (Technical Specifications of Ukraine 48-10-93-88)

  Mg(II) powder 325 mesh (HyperTec, USA)

(II) *ex-situ* from MgB_2 powder

- ✓ Magnesium diboride (98% purity)